

THE ECONOMIC IMPACT OF LOW- AND HIGH-FREQUENCY TEMPERATURE CHANGES

Nikolay Gospodinov*

Ignacio Lopez Gaffney[†]

Serena Ng[‡]

June 10, 2025

Abstract

Temperature data have low- and high-frequency variations that may have distinct impacts on economic outcomes. Analyzing data from a panel of 48 states in the U.S., and a panel of 50 countries, we find slowly evolving, low-frequency components with periodicity greater than 32 years. These components have a common factor that trended up around the same time that economic growth slowed. Panel regressions using U.S. data fail to find a statistically significant impact of low-frequency temperature changes on growth, though the impact of high-frequency temperature changes is marginally significant. However, using the international panel (which includes several European countries), we find that a 1°C increase in the low-frequency component is estimated to reduce economic growth by about one percent in the long run. Though the first-order effect of high frequency changes is not statistically significant in this data, a smaller non-linear effect is detected. Our estimation and inference procedures control for common, business cycle variations in output growth that are not adequately controlled for by an additive fixed effect specification. These findings are corroborated by time series estimation using data at the unit and national levels.

Keywords: Global warming; Economic growth; Low-frequency components and co-variability; High-frequency changes; Panel data; Cross-sectional heterogeneity.

JEL Classification: O44, Q54, C22, C23.

*Federal Reserve Bank of Atlanta, Email: nikolay.gospodinov@atl.frb.org

[†]Department of Economics, Yale University and Yale Law School, Email: ignacio.gaffney@gmail.com

[‡]Corresponding author: Department of Economics, Columbia University and NBER. 420 W. 118 St. New York, NY 10027. Email: serena.ng@columbia.edu

This work is supported by the National Science Foundation (SES: 2018369). The views expressed in this paper are those of the authors and do not necessarily represent those of the Federal Reserve Bank of Atlanta or the Federal Reserve System.

1 Introduction

Average global temperatures have increased by 0.11°F per decade since 1850 – or about 2.2°F in total – with warming occurring three times faster since 1982.¹ Non-seasonal increases in temperature can arise because of heat waves, or because of El Niño and La Niña, which shift climate patterns in the Pacific Ocean roughly every 3-7 years. Variations can also occur due to solar cycles that flip the sun’s magnetic field every 11 years, as well as alternating periods of cool-damp and warm-dry weather related to 35-year Bruckner cycles.² The possible existence of temperature variations with different periodicities will affect how we model the economic impact of environmental changes and how we design mitigation policies. It is also of economic interest to understand how agents distinguish the different types of variations from the data.

The literature often treats weather – atmospheric conditions over short periods of time – as conceptually distinct from climate, represented by moments of weather variables computed over a long sample (e.g., IPCC (2014)). Of concern are persistent changes to the climate. We focus on persistent variations in one weather variable – temperature – modeling observed temperature X as the sum of two unobserved components: one of ‘low’ frequency denoted \mathcal{L}_X^0 (akin to climate), and one of ‘high’ frequency denoted \mathcal{H}_X^0 (akin to weather). In a stationary environment, \mathcal{L}_X^0 would be the constant, long-run mean, and \mathcal{H}_X^0 would be a series of deviations from this constant. To capture non-stationarity, we allow \mathcal{L}_X^0 to be a slowly evolving process, possibly with long memory.

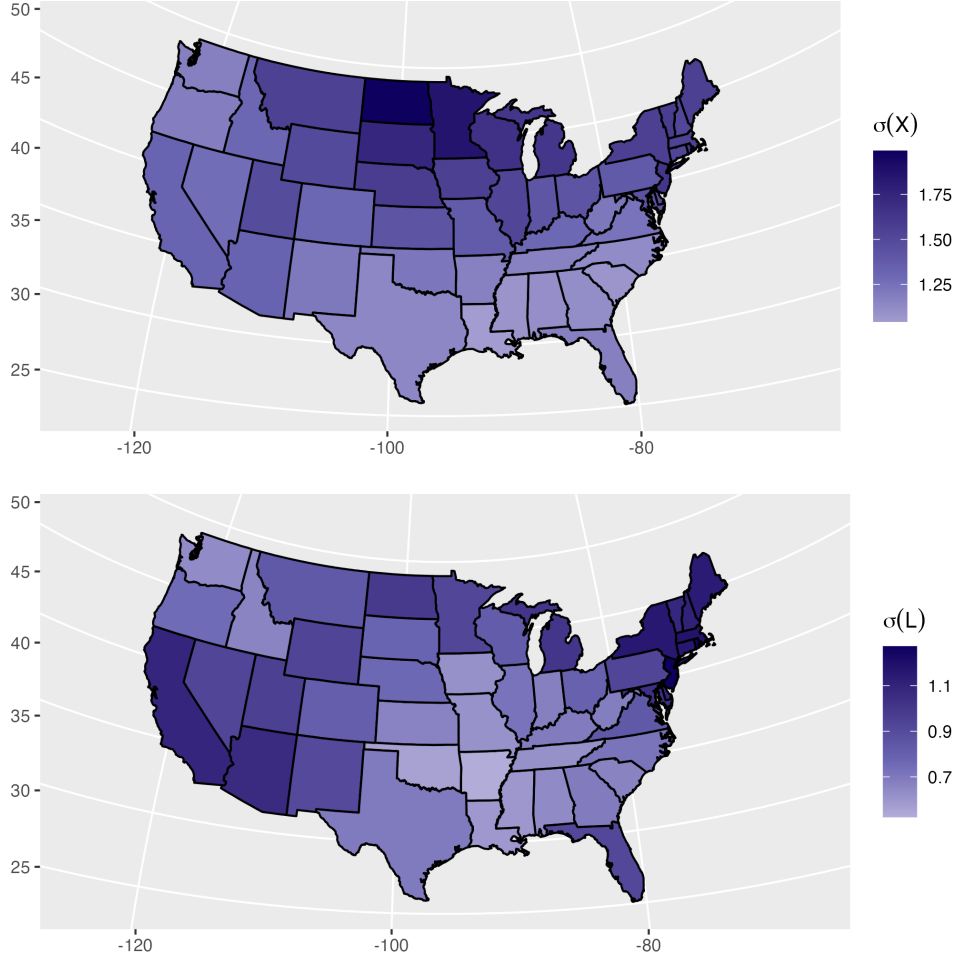
To appreciate why it is useful to separate temperature data X into two components, consider annual temperature for the 48 contiguous states in the U.S. The top panel of Figure 1 shows the standard deviation of X for each state over the sample 1895-2023. At face value, the plot suggests that variability in temperature is more pronounced in the middle of the country. Now consider the bottom panel of Figure 1 which shows the standard deviation of $\hat{\mathcal{L}}_X$, where $\hat{\mathcal{L}}_X$ is based on the MWq Mueller and Watson (2008) low-frequency estimator with $q = 8$ (which will be discussed extensively below). With $T = 129$, $\hat{\mathcal{L}}_X$ captures variations with periodicity longer than $2T/q \approx 32$ years. Unlike the top panel, this figure indicates that low-frequency variations in the U.S. are stronger along the coasts, while the high-frequency variations are stronger in the interior. As we will see below, spatial differences in the concentration of the two components are also found in an international panel spanning 1952-2018.

Recognizing spatial differences in the concentration of the two components is especially

¹<https://www.climate.gov/news-features/understanding-climate/climate-change-global-temperature>

²https://en.wikipedia.org/wiki/Eduard_Bruckner.

Figure 1: U.S. Heatmap of $\sigma(X)$ and $\sigma(\hat{\mathcal{L}}_X)$ (1895–2023)

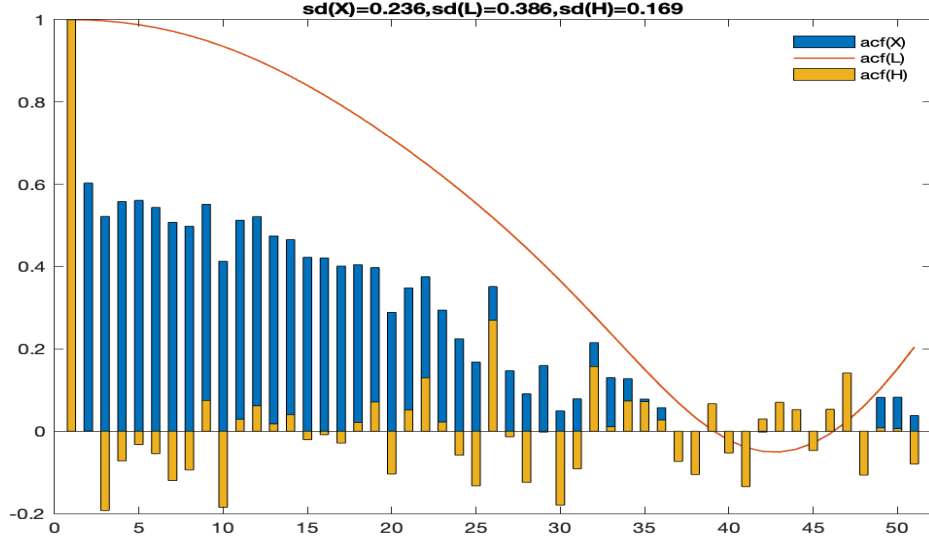


The top panel plots the standard deviations of temperature for 48 states in the U.S. The bottom panel plots the standard deviations of the corresponding low-frequency components estimated by MWq with $q = 8$.

important due to their vastly different dynamic properties. To illustrate this point, Figure 2 plots the correlogram for X (in blue), $\hat{\mathcal{L}}_X$ (in red), and the high-frequency component $\hat{\mathcal{H}}_X$ (in brown), at the national level for the United States. The autocorrelation function of $\hat{\mathcal{L}}_X$ decays very slowly and declines to zero after 30–35 years. This is in line with our choice of $q = 8$, which generates a $\hat{\mathcal{L}}_X$ with periodicity of at least 32 years. We also notice that X is less persistent than $\hat{\mathcal{L}}_X$, which follows from the fact that $\hat{\mathcal{H}}_X$ – which exhibits short memory – is included in X . Since shocks to $\hat{\mathcal{L}}_X$ will last much longer than shocks to $\hat{\mathcal{H}}_X$, this motivates us to estimate the economic effects of \mathcal{L}_X^0 and \mathcal{H}_X^0 separately.

As \mathcal{L}_X^0 is not observed, we explore different ways of estimating it and study the properties of those estimators $\hat{\mathcal{L}}_X$ using our U.S. panel. We begin by fitting a parametric unobserved

Figure 2: Correlogram of National Temperature X , $\hat{\mathcal{L}}_X$ and $\hat{\mathcal{H}}_X$



$\hat{\mathcal{L}}_X$ series is constructed from the MW8 procedure, and $\hat{\mathcal{H}}_X = X - \hat{\mathcal{L}}_X$. With $T = 129$, the standard error under the null hypothesis of no autocorrelation is $\frac{1}{\sqrt{T}} = 0.088$.

components model with long memory to X_i for each $i = 1, \dots, N$ in the panel. The estimates suggest significant spatial differences in the variability of $\hat{\mathcal{L}}_{X_i}$ relative to $\hat{\mathcal{H}}_{X_i}$. The $\hat{\mathcal{L}}_{X_i}$ series has been trending up in recent decades and appears non-linear over the full sample. The upward trend coincides with a downward trend in $\hat{\mathcal{L}}_Y$, the low-frequency component of economic growth. Further investigation finds that there is a strong common factor in the panel of $\hat{\mathcal{L}}_X$, but the loadings are heterogeneous across geographic units. These features are corroborated by three trend estimators used in economic analysis, and by data at the national level. A Monte Carlo exercise calibrated to temperature data finds that with the ‘right’ hyperparameter, all methods provide a similar approximation to \mathcal{L}_X^0 . We continue the analysis with the MWq procedure because its estimates of $\hat{\mathcal{L}}_X$ and $\hat{\mathcal{H}}_X$ are relatively insensitive to the choice of tuning parameter and are orthogonal by construction.

To quantify the conditional covariability between the components of temperature and economic growth, we turn to regressions. Most estimates of the economic impact of warming temperatures are based on additive fixed effect panel regressions, and rely on clustered standard errors that do not control for time dependence in the residuals. Our regression analysis differs in three ways. First, we study the distinct impacts of low- and high-frequency compo-

nents of temperature on economic growth. Second, we use two-way (unit and time) clustered standard errors to guard against the possibility that the additive fixed effect specification may not adequately control for common unobserved heterogeneity in the time dimension. Third, we entertain an interactive fixed effects specification, and develop a bootstrap that delivers reliable coverage properties of the constructed confidence intervals while preserving three salient features of the data: long memory in the low-frequency components, unobserved heterogeneity with a common factor that aligns with economic conditions, and notable spatial variations in the loadings.

The main departure of our regression analysis from existing work is that we allow \mathcal{L}_X^0 and \mathcal{H}_X^0 to have different impacts on the economy. To gain some intuition, consider an X_t that is a random walk. Then, $\mathcal{L}_{X,t}^0 = X_{t-1}$ and $\mathcal{H}_{X,t}^0 = \Delta X_t$. We would expect the regression coefficients from ΔY on ΔX to differ from those from ΔY on X , as X includes low-frequency variations, while differencing removes any zero-frequency variations from ΔX . And yet, since $X = \mathcal{L}_X^0 + \mathcal{H}_X^0$, the regression $\Delta Y = c + \beta_X X + u$ imposes the restriction that $\beta_{\mathcal{H}}$ – the effect of a change to the high-frequency component – be the same as $\beta_{\mathcal{L}}$ – the effect of a change to the low-frequency trend. As $\text{cov}(X, \Delta Y) = \beta_{\mathcal{L}} \text{var}(\mathcal{L}_X^0) + \beta_{\mathcal{H}} \text{var}(\mathcal{H}_X^0)$, the population parameter β_X is

$$\beta_X = \beta_{\mathcal{L}} \frac{\text{var}(\mathcal{L}_X^0)}{\text{var}(X)} + \beta_{\mathcal{H}} \frac{\text{var}(\mathcal{H}_X^0)}{\text{var}(X)}.$$

To the extent that \mathcal{L}_X^0 is non-stationary, β_X should tend to $\beta_{\mathcal{L}}$ as $T \rightarrow \infty$. But in finite samples, the least squares estimate $\hat{\beta}_X$ will be a weighted sum of $\beta_{\mathcal{L}}$ and $\beta_{\mathcal{H}}$ (unless the low-frequency variations dominate). Furthermore, the autocovariance structure of X is a non-linear function of those of its components, \mathcal{L}_X^0 and \mathcal{H}_X^0 , so the dynamic response of X will also depend on which component is being perturbed.³

Regressions using the U.S. panel over the 1964–2023 sample find a significant and negative $\hat{\beta}_{\mathcal{L}}$ that is different from $\hat{\beta}_{\mathcal{H}}$, but only under the assumption that there are no common year effects. Even in this model, the estimates deemed statistically significant according to one-way clustered standard errors become insignificant using two-way clustering. The additive and (less restrictive) interactive fixed effect estimators – which control for common year effects relating to the business cycle – both result in a $\hat{\beta}_{\mathcal{L}}$ that is not statistically different from zero. Therefore, even though $\hat{\mathcal{L}}_X$ increased by 3.046°F between 1964 and 2023, its impact on economic growth in the U.S. does not seem to be credible.

The evidence from a panel of 20 European countries, and an international panel of 50

³Even in the simple case when \mathcal{L}_X is a random walk and \mathcal{H}_X is an AR(1), ΔX will be an ARMA(1,1).

countries with wide geographic coverage and variation in incomes, is more supportive of a negative effect of $\hat{\mathcal{L}}_X$ on ΔY . Based on interactive fixed effect regressions, we estimate a coefficient for $\hat{\mathcal{L}}_X$ of -0.947 in the European panel and -1.401 in the international panel. Considering that the cross-sectional average of $\hat{\mathcal{L}}_X$ in Europe has increased by 1.471°C (or a population-weighted average of 1.480°C) in the 38 years between 1980 and 2018, the annual impact on GDP growth is about 4 basis points.

The economic impact of high-frequency temperature variations also differs between the U.S. and Europe. While the first-order impact of $\hat{\mathcal{H}}_X$ in the U.S. panel is -0.145 and marginally significant, this effect is negative, but not significant, in the European or international panels. However, there is some evidence of a nonlinear effect in these data when the marginal effect of the high-frequency component is allowed to vary with the low-frequency component. This effect is small and does not change the conclusion that the high- and low-frequency components have different economic impacts, and that these impacts differ in the U.S. and Europe. In short, there is limited evidence that high-frequency variations drive the relationship between temperature and output growth in the U.S., while low-frequency components play a dominant role in the European and international panels.

While recent work on this topic has mostly focused on estimates from panel regressions, we also perform time series regressions using unit-level and aggregate data. These regressions lead to the same conclusion that the long-run impact of the low-frequency component in the U.S. on growth is not statistically different from zero. The aggregate estimate for European countries also corroborate the panel data results of a significant negative relationship between the low-frequency components of temperature and growth, although the estimated effect from the aggregate time-series regression is even larger than the one obtained from the panel regressions. As there is no need to control for heterogeneity in this setting – as in panel regressions – there is some appeal to looking for aggregate evidence from time series regressions, especially as we gain more time series observations going forward.

The rest of the paper proceeds as follows. Section 2 uses a structural dynamic model to motivate the decomposition of X into high- and low-frequency components. It also reviews several non-parametric estimators of these latent processes, and characterizes the common and idiosyncratic variations in X and ΔY for the U.S. panel. Section 3 uses regressions to estimate the average and state/country level effects of the components of X on ΔY . Section 4 concludes.

Data: In this paper, we use data from two panels. The U.S. panel consists of data for the 48 contiguous states. Temperature data is available for the 1895-2023 sample, while the growth rate of real per capita Gross State Product (GSP) is available for the 1964-2023 sample.⁴ The international panel consists of data for 50 countries. Temperature data is available for the 1901-2022 sample, while the growth rate of real per capita GDP is available for the 1953-2018 sample. A European panel is also constructed from this international panel. A detailed description of the data is provided in Appendix A.

We construct temperature series as deviations from their pre-1980 mean. This data transformation allows all series to have approximately the same level, and facilitates comparison across geographic units. We will often refer to ‘national’ or ‘aggregate’ temperature series, which are defined as population-weighted averages of unit temperature series.

2 Modeling \mathcal{L}^0

The notion of low-frequency variations is important in our analysis, so it is useful to be clear on what we are studying. A series with T observations can emerge from different configurations of the sampling frequency and span of the data. For example, $T = 120$ observations can be obtained from collecting annual data over 120 years, or over a shorter span of 10 years but with data sampled at the monthly frequency. For a given sampling frequency and span, our point of departure is that a time series can be expressed as a sum of orthogonal components each isolating variations with a different periodicity (e.g., Harvey (1994, Chapter 6)). Component j has periodicity $p_j = \frac{2\pi}{\omega_j}$ if it repeats itself every p_j periods, where $\omega_j \in [0, \pi]$ is the frequency at which the spectral density has notable mass. For economic time series, such as the inflation rate, focus is usually on the business cycle component, which has periodicity between 6 and 32 quarters.

Temperature data, likewise, have variations at different frequencies that are of interest. We work with annual data, which are void of variations at seasonal frequencies⁵ to focus on the low-frequency component trend \mathcal{L}_X^0 (i.e., the trend attributable to variations at zero or near-zero frequencies). With some abuse of terminology, we will refer to $X - \mathcal{L}_X^0 \equiv \mathcal{H}_X^0$ as the high frequency component, even though these variations may still be persistent. The crucial distinction is when ω_j is near zero, the periodicity is high. Our goal is to

⁴We also considered quarterly (seasonally adjusted) data for the 1948Q1–2023Q4 period. The findings are qualitatively similar.

⁵Hsiang and Burke (2014) suggest that analysis of data over a long span may suffer from a “frequency-identification tradeoff” if society changes at a faster rate than low-frequency changes in climate. The statement is as much about the span of the data as it is about low-frequency variations themselves.

study the properties of the low-frequency component at the state/country level, and at the aggregate level. Though simple trend functions and filters have been used to represent the low-frequency component of temperature before, these procedures have not been studied in a systematic manner.⁶ Trend-cycle decomposition is, however, a well-studied problem in the economics literature. We leverage this knowledge to analyze the low-frequency component of temperature data by first using a parametric model to gain insights about its underlying persistence, and by then using other non-parametric ways to isolate it.

2.1 An Unobserved Components Model with Long Memory

For a generic variable Z_t observed for $t = 1, \dots, T$, an unobserved components model posits that

$$Z = \mathcal{L}^0 + \mathcal{H}^0.$$

We observe Z but not the two latent components. The standard UC model parameterizes \mathcal{H}^0 as a covariance stationary process and \mathcal{L}^0 as an $I(d)$ process with d taking on integer values of one or two. When Z is economic output, Beveridge and Nelson (1981) and Kuttner (1994) associate \mathcal{L}^0 with potential output, while Clark (1987) associates \mathcal{H}^0 with the business cycle. Marino and Marmol (2004) and more recently, Hartl (2023) relax the assumption that d is integer valued. This more flexible model entertains the possibility that temperature data has long memory, as documented in Mills (2007), Gil-Alana et al. (2022), Yuan et al. (2014), among others.

The low- and high-frequency components are assumed to evolve according to

$$\begin{aligned} (1 - L)^d \mathcal{L}_t^0 &= \epsilon_{\mathcal{L},t}, & \epsilon_{\mathcal{L},t} &\sim (0, \sigma_{\mathcal{L}}^2), \\ \mathcal{H}_t^0 &= a(L) \epsilon_{\mathcal{H},t}, & \epsilon_{\mathcal{H},t} &\sim (0, \sigma_{\mathcal{H}}^2), \end{aligned}$$

where $a(L) = 1 + a_1 L + \dots + a_p L^p$. Let $b(L) = a(L)^{-1} = \sum_{j=0}^{\infty} b_j L^j$. Assuming that $\sum_{j=0}^{\infty} |b_j|$ is bounded, and bounded away from zero, Hartl (2023) shows that optimal filtering yields

$$\begin{aligned} \mathcal{L}_{t:1}(Z_{t:1}, \psi) &= (B_t' B_t + \nu S_t' S_t)^{-1} B_t' B_t Z_{t:1}, \\ \mathcal{H}_{t:1}(Z_{t:1}, \psi) &= \nu (B_t' B_t + \nu S_t' S_t)^{-1} S_t' S_t Z_{t:1}, \end{aligned}$$

⁶See, for example, Wu et al. (2007), Mills (2007), Mudelsee (2019), Kaufmann et al. (2013) for an analysis of non-stationarity. Zhang et al. (2007) use a 40 year Butterworth filter to look for patterns between wars and temperature changes, while Tol and Wagner (2010) use a 10-year Hamming window. Bastien-Olvera et al. (2022) remove variations with periodicity up to 15 years. Hsiang (2016) uses the band-pass filter with different cut-offs to analyze variations in corn yields, but effectively remove the low-frequency variations that are of focus here.

where $\nu = \sigma_{\mathcal{H}}^2/\sigma_{\mathcal{L}}^2$, S_t and B_t are upper triangular Toeplitz matrices.⁷ Both \mathcal{L}^0 and \mathcal{H}^0 depend on the known parameters $(\sigma_{\mathcal{H}}, \sigma_{\mathcal{L}}, d, a_1, \dots, a_p)$.

Let $\hat{\mathcal{L}}_X$ and $\hat{\mathcal{H}}_X$ be estimates of the components of temperature X when the parameters are estimated by maximum likelihood.⁸ Our estimation with $p = 1$ finds $\hat{\sigma}_{\mathcal{L}}$ to be small. This is concerning because even in the standard UC model when d is fixed at 1, identification is challenging when $\sigma_{\mathcal{L}}/\sigma_{\mathcal{H}}$ is small.

Therefore, we fix $\sigma_{\mathcal{L}}$ to take on values between 0.01 and 0.5 and estimate only the remaining parameters, $(\sigma_{\mathcal{H}}, d, a_1)$. While the likelihood is maximized at $\sigma_{\mathcal{L}} = 0.04$, it is similar for any $\sigma_{\mathcal{L}} \in [0.04, 0.4]$. Notably, $\hat{\mathcal{L}}_X$ is more variable when $\sigma_{\mathcal{L}} = 0.4$ than when $\sigma_{\mathcal{L}} = 0.04$, but have similar autocorrelations. Importantly, the findings that there is significant dispersion in $\hat{\sigma}_{\mathcal{H}}$ across states, and \hat{d} always exceeds 0.5 – making $\hat{\mathcal{L}}_X$ non-stationary – hold for any $\sigma_{\mathcal{L}} \in [0.04, 0.4]$.

In view of the near equivalence of second moment properties of the filtered series $\hat{\mathcal{L}}_X$ in the parameter space of interest, we can analyze a series associated with any $\sigma_{\mathcal{L}}$ in the range $[0.04, 0.4]$. Hereafter, we will denote a UC model with $\sigma_{\mathcal{L}}$ fixed at ω as UC ω . Table 1 shows results ordered by $\hat{\sigma}_{\mathcal{H}}$ for $\sigma_{\mathcal{L}} = 0.2$. Also reported is $\Delta\mathcal{L}_X = \hat{\mathcal{L}}_{X,T} - \hat{\mathcal{L}}_{X,1}$, the change in the low-frequency component over the sample. The states with the largest $\hat{\sigma}_{\mathcal{H}}$ (e.g., ND, MN, SD, IA, WI) are located in the middle of the country. The states with the lowest $\hat{\sigma}_{\mathcal{H}}$ (e.g., FL, CA, SC, LA, NC) are warm and coastal, and also exhibit the largest change in $\hat{\mathcal{L}}_X$. The population-weighted average of the parameters $(\hat{d}, \hat{a}_1, \hat{\sigma}_{\mathcal{H}}, \hat{\nu})$ are (1.039, 0.137, 0.974, 24.990), with cross-sectional standard deviations of (0.056, 0.107, 0.263, 16.271). The national estimates are (1.019, 0.201, 0.628, 9.886). Both the state-level and national estimates find weak persistence in $\hat{\mathcal{H}}_X$. The national $\hat{\sigma}_{\mathcal{H}}$ of 0.628 is lower than the aggregate estimate of 0.974, as averaging the data prior to estimation reduces noise. Note that with $\sigma_{\mathcal{L}} = 0.2$, the \hat{d} s are all less than 1.5 at the state level, while \hat{d} is close to 1 at the national level. This aligns the national data closely with the standard UC model, where $d = 1$. Both features are appealing for subsequent analysis.

An interesting aspect of the UC model is that when $t = T$, $d = 2$, and $b(L) = 1$, $\hat{\mathcal{L}}_X$ is equivalent to the Hodrick-Prescott (HP) filter, with ν serving as a smoothing parameter denoted as λ . For quarterly economic data, a λ of 1600 is found to roughly isolate business cycle variations (i.e., those with periodicity between 6 and 32 quarters). Ravn and Uhlig (2002) suggest setting λ to 6.25 when using annual data to obtain a cyclical component

⁷The S_t matrix is a function of $(\pi_0(d), \pi_1(d), \dots, \pi_{t-j}(d))$, $\pi_j(d) = \frac{j-d-1}{j}\pi_{j-1}(d)$ starting with $\pi_0(d) = 1$, and the B_t matrix has $(b_0, b_1, \dots, b_{t-j})$ in the j th-row, respectively.

⁸Hartl (2023) allows a_j to depend on parameters φ . For our purpose, it suffices to remove this generality.

Table 1: Annual Temperature of States Ordered by $\sqrt{\hat{\nu}} = \hat{\sigma}_{\mathcal{H}}/\sigma_{\mathcal{L}}$

State	\hat{d}	1895-2023			State	\hat{d}	$T = 129$ $\sigma_{\mathcal{L}} = 0.2$			State	\hat{d}	$\Delta^h \hat{\mathcal{L}}_X$ $\hat{\sigma}_{\mathcal{H}}$		
		$\Delta^h \hat{\mathcal{L}}_X$	$\hat{\sigma}_{\mathcal{H}}$				$\Delta^h \hat{\mathcal{L}}_X$	$\hat{\sigma}_{\mathcal{H}}$				$\Delta^h \hat{\mathcal{L}}_X$	$\hat{\sigma}_{\mathcal{H}}$	
Bottom third				Middle Third				Top Third						
FL	1.002	3.156	0.716	WA	0.839	1.611	0.989	UT	0.967	2.558	1.149			
CA	0.991	2.778	0.737	TN	0.912	1.472	0.998	VT	1.028	3.233	1.160			
AZ	0.964	2.670	0.780	MA	1.059	3.712	0.999	WY	0.925	2.116	1.189			
NM	0.979	2.542	0.798	CT	1.027	3.486	1.003	OH	0.946	2.218	1.201			
SC	0.933	1.796	0.847	MD	1.013	3.090	1.010	MO	0.824	1.339	1.260			
LA	0.902	1.661	0.860	NJ	1.044	3.792	1.017	IN	0.878	1.604	1.271			
NC	0.963	1.992	0.869	WV	0.942	1.762	1.017	KS	0.835	1.363	1.286			
NV	0.953	2.204	0.873	CO	0.902	1.999	1.021	MI	0.983	2.787	1.304			
GA	0.970	1.873	0.874	PA	0.981	2.801	1.031	MT	0.904	1.906	1.340			
AL	0.945	1.466	0.905	NH	1.029	3.371	1.044	IL	0.878	1.750	1.369			
MS	0.922	1.468	0.910	NY	1.018	3.376	1.055	NE	0.873	1.545	1.418			
TX	0.928	2.090	0.914	AR	0.799	0.927	1.071	WI	0.916	2.035	1.473			
OR	0.879	1.922	0.917	ME	1.020	3.268	1.074	IA	0.776	1.041	1.476			
VA	0.984	2.516	0.923	KY	0.940	1.728	1.113	SD	0.844	1.475	1.586			
RI	1.065	3.759	0.974	OK	0.826	0.931	1.113	MN	0.921	2.095	1.647			
DE	1.014	3.225	0.979	ID	0.850	1.562	1.137	ND	0.898	1.860	1.768			

X is the deviation of temperature (in Fahrenheit) from the pre-1980 mean. $\Delta^h \hat{\mathcal{L}}_X = \hat{\mathcal{L}}_{X,2023} - \hat{\mathcal{L}}_{X,1895}$, $\hat{\mathcal{L}}_X$ is estimated by the UC model with $\sigma_{\mathcal{L}} = 0.2$, \hat{d} is the long memory parameter, and $\hat{\sigma}_{\mathcal{H}}$ is the innovation variance of \mathcal{H}_X parameterized as an AR(1).

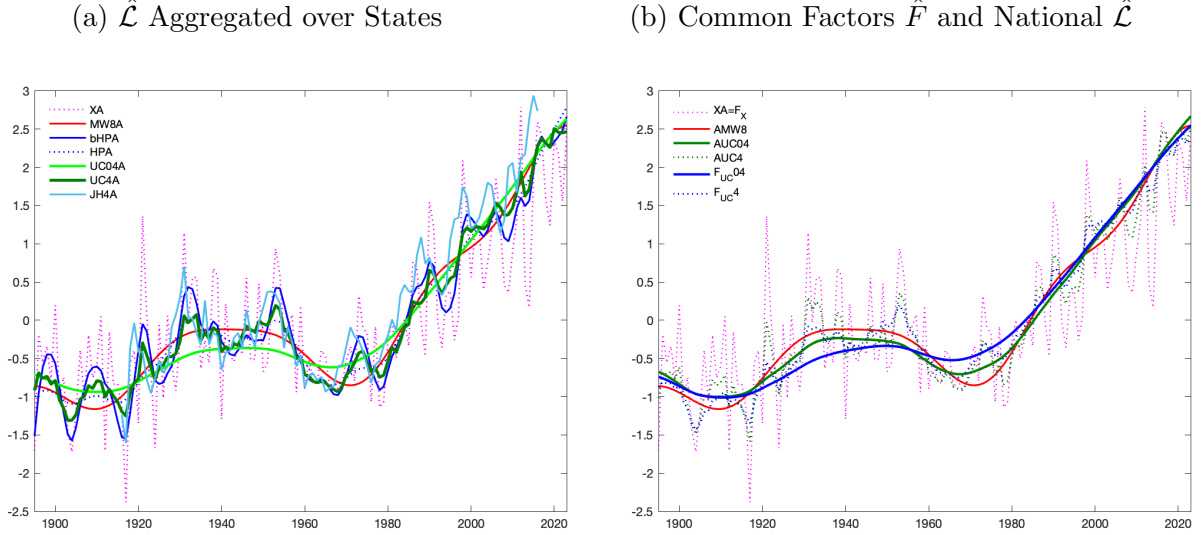
with similar spectral properties. Our \hat{d} s are well below 2, and the $\hat{\nu}$ s are well above 6.25, suggesting that a λ suitable for economic data is not appropriate for analyzing the low-frequency component of X , an issue that will be further investigated in the next subsection.

A stark conclusion of this analysis is that, based on the parameters suggested by the data, $\hat{\mathcal{L}}_X$ is strongly persistent and decisively non-stationary, which means it will not mean-revert after an increase in $\epsilon_{\mathcal{L}}$. In contrast, $\hat{\mathcal{H}}_X$ is nearly white noise and will quickly return to its mean after an increase in $\epsilon_{\mathcal{H}}$. Thus, if $\hat{\mathcal{L}}_X$ is found to co-vary with economic outcomes, changes in $\hat{\mathcal{L}}_X$ will have long-lasting effects. Before proceeding to such an analysis, we need to verify that the strong persistence of $\hat{\mathcal{L}}_X$ is not specific to the estimates of the UC model.

2.2 Alternative Decompositions

Given the near observational equivalence of many configurations of (d, ν) , pinning down the ‘best’ parametric model is futile. Nevertheless, if we only require an estimate of \mathcal{L}_X^0 to analyze

Figure 3: Estimates of \mathcal{L}_X using MW, HP, and JH.



The figure presents U.S. aggregate temperature data XA (as deviation of temperature (in Fahrenheit) from its pre-1980 mean) and various estimates of the low-frequency component \mathcal{L}_X , described in the text.

its impact on the economy, it may suffice to adequately approximate \mathcal{L}_X^0 without knowing its precise structure. In this subsection, we consider trend-filtering procedures used in economic analysis. Each procedure requires tuning parameters, so we may think of $\mathcal{L}_X = \mathcal{L}_X^0 + a_{\mathcal{L}}$, where $a_{\mathcal{L}}$ is an approximation error. In practice, \mathcal{L}_X has to be estimated, and $\hat{\mathcal{L}}_X$ will have both an approximation and a sampling error.

We consider three procedures: JH(p,h), HP(λ) or bHP, and MWq. The first is the JH(p,h) procedure of Hamilton (2018), which does not require knowledge of whether d is 0, 1, or 2. The second is the HP(λ) filter of Hodrick and Prescott (1997), and an improved bHP(λ) developed by Phillips and Jin (2021) and Phillips and Shi (2021). The third is the MWq procedure developed in Mueller and Watson (2008, 2017, 2022).

MWq generates a low-frequency component of an arbitrary time series Z with periodicity longer than $2T/q$ by projecting Z on a constant and q periodic functions collected into $\Psi_T = (\Psi_1, \dots, \Psi_q)'$, where $\psi_j(s) = \sqrt{2} \cos(js\pi)$ for $j = 1, \dots, q, s = (t - 1/2)/T$, for $t = 1, \dots, T$. Figure 1 in the Introduction is based on MW8. Mueller and Watson (2016) show that the procedure is valid for (b,c,d) processes with spectrum $S(\omega) \propto (\omega^2 + c^2)^{-d} + b^2$ for $-1/2 < d < 3/2$. It approximates \mathcal{L}_X^0 without knowledge of b, c , or d and nests the local-to-unity model and the local-level model as special cases.

For each method considered, we will refer to two different but related estimates of aggregate $\hat{\mathcal{L}}_X$. When we form aggregate estimates from a weighted sum of state-level estimates

$\hat{\mathcal{L}}_X = \sum_{i=1}^N \omega_i \hat{\mathcal{L}}_{X,i}$ (where ω_i are population weights), these estimates will be denoted with a label that ends with ‘A’. When we form an aggregate (or national) series $AX = \sum_{i=1}^N \omega_i X_i$, and then apply an estimation method, the label will start with ‘A’. For example, AMW8 is obtained by applying the MW procedure with $q = 8$ to the aggregate series, while MW8A is obtained by aggregating the 48 state-level estimates based on MW8. Similarly, UC04A is obtained by aggregating the UC estimates with $\sigma_{\mathcal{L}}$ fixed at 0.04, while AUC04 is obtained by applying the estimation method to the aggregate series with the same $\sigma_{\mathcal{L}}$.

The left panel of Figure 3 presents the aggregate of state-level estimates. For the sake of facilitating comparison, all estimates are standardized to have zero mean and unit variance. In brief, the MW8A, HPA(100), and UC04A are similarly smooth, while bHPA, UC4A, and JH4A, are more variable. However, all estimates trend upward over the course of the sample. A detailed analysis of the properties of these estimates is provided in Appendix B.

The procedures considered are designed for filtering of economic data. We do not know how accurate they are for estimating temperature trends, and for this, we need to know the true low-frequency component, which is never observed. We thus design a Monte-Carlo exercise, calibrated to several temperature series, to evaluate the total (approximation plus sampling) mean-squared error of the procedures. The simulation exercise, also detailed in Appendix B, reveals that though the tuning parameters used to obtain economic trends or cycles are not appropriate for estimating the low- and high- frequency components of temperature data, any of the methods can produce a similar trend with the right choice of tuning parameter. This suggests that the issue, then, is to decide on a robust choice of tuning parameters.

In our experience, the MW procedure is relatively insensitive to the choice of tuning parameters, and is therefore quite robust. For example, MW16 performs better than MW8 when $\sigma_{\mathcal{L}} = 0.4$. As the underlying \mathcal{L}_X^0 is more variable, a larger q provides a better approximation of the low-frequency component. However, even with $q = 8$, the RMSE of MW8 is remarkably stable. The MW procedure has other properties that make it attractive. For one, the same q can be used to generate a similar $\hat{\mathcal{L}}_X$ whether we work with monthly, quarterly, or annual data. In addition, the procedure is invariant to aggregation, meaning that AMW8 is the same as MW8A. Lastly, the MW trend is easy to interpret, as we only need to map q to a certain periodicity to understand which atmospheric cycles of interest are captured in the estimate. In what follows, we choose a q so that for given T , the MW q estimate of \mathcal{L}_X has periodicity greater than 32 years.

The MW q procedure is also useful to learn more about $\hat{\mathcal{H}}_X$. Because $\hat{\mathcal{H}}_X$ is too volatile

to be visually informative, we apply the MWq procedure with a large q in search of insights. With $T = 129$, a q of 56 and 26 would correspond to a periodicity of 4.60 and 7.16 years, respectively. The national estimate of \mathcal{H}_X is roughly sandwiched by AMW26 and AMW56. Given that the ENSO (El Niño–Southern Oscillation) effects are irregular cycles that recur every 2 to 7 years,⁹ the data suggest an ENSO component in $\hat{\mathcal{H}}_X$.

2.3 Common and Idiosyncratic Low-Frequency Variations

The finding that most states have a trending $\hat{\mathcal{L}}_{X,i}$ raises the question of whether these variations are common or state-specific. We construct the first principal component, denoted F_X , $F_{\mathcal{L}}$, and $F_{\mathcal{H}}$, from X , $\hat{\mathcal{L}}_X$, and $\hat{\mathcal{H}}_X$, respectively. The first two are shown in the right panel of Figure 3.

Three features are of note. First, while F_X in this data is indistinguishable from the aggregate data XA (equivalently, AX), it is noticeably different from $F_{\mathcal{L}}$, which is smoother. Second, estimates of \mathcal{L}_X using AX are similar to aggregated sub-national estimates. This can be seen by comparing AUC04 with UC04A, and AMW8 with MW8A. Therefore, if one is solely interested in an economy-wide estimate of the low-frequency component, it suffices to go top-down and estimate it directly from national data. Third, regardless of the method that is used, aggregate estimates of $\hat{\mathcal{L}}_X$ are relatively constant between 1895 and 1963, and trend up thereafter. This is important because we will be analyzing the relationship between economic outcomes and $\hat{\mathcal{L}}_X$ in this latter period, where the series seems to behave like a linear trend.

As explained in Mueller and Watson (2018), variations in \mathcal{L}_X over time are due entirely to the $q \ll T$ vector $\mathbb{X} = T^{-1}\Psi'_T X$, and similarly for ΔY . Because q is small, inference on \mathcal{L}_X becomes a small sample problem. To make inferences on common variations at low-frequency, we adapt the framework of Foerster et al. (2022) which demonstrates that low-frequency data admit a factor representation¹⁰:

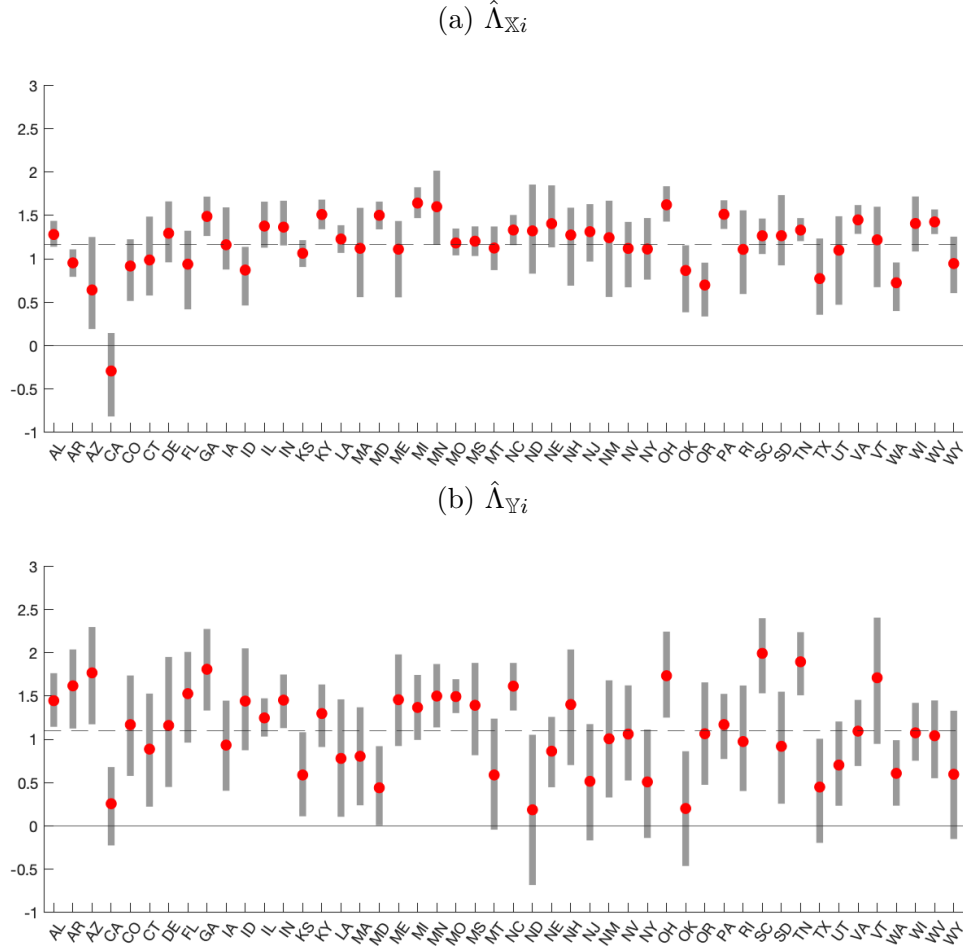
$$\begin{pmatrix} \mathbb{X}_i \\ \Delta \mathbb{Y}_i \end{pmatrix} = \begin{pmatrix} \Lambda'_{\mathbb{X}i} I_q & 0 \\ 0 & \Lambda'_{\mathbb{Y}i} I_q \end{pmatrix} \begin{pmatrix} \mathbb{F}_1 \\ \mathbb{F}_2 \end{pmatrix} + \begin{pmatrix} U_X \\ U_Y \end{pmatrix}.$$

We estimate \mathbb{F} and the Λ matrices using the Bayesian procedure explained in Mueller and Watson (2022) to facilitate small sample inference, even though the Bayesian estimates of \mathbb{F} are similar to the principal component estimates shown earlier.

⁹Data source: https://psl.noaa.gov/enso/enso_101.html

¹⁰The X in Foerster et al. (2022) is labor input and ΔY is sectoral TFP.

Figure 4: Estimates of Covariability and Factor Loadings by State



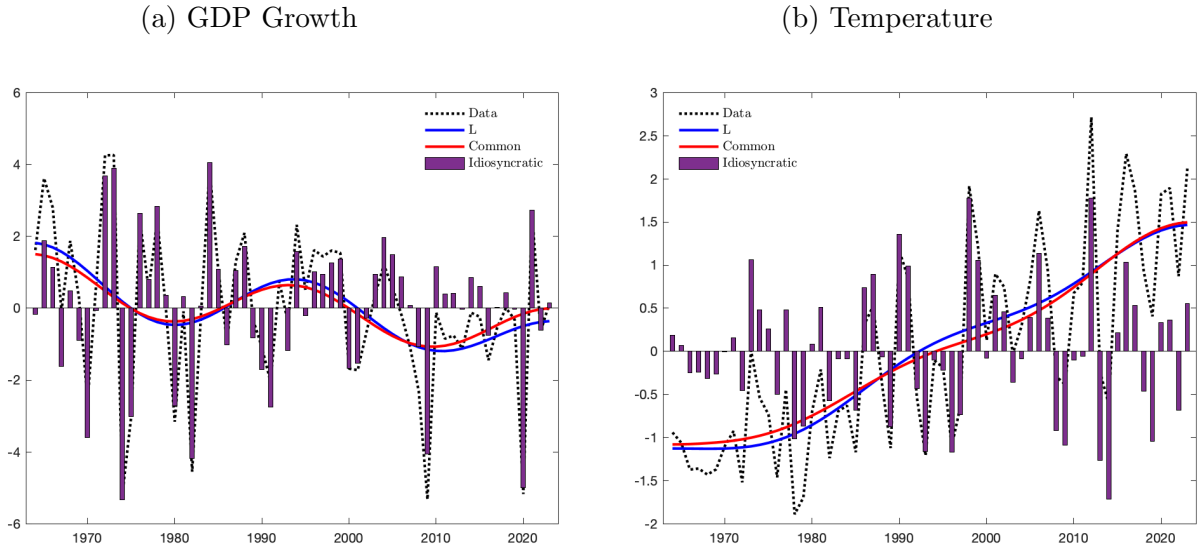
This figure presents estimates (red dots) by state, corresponding 68% credible sets (shaded gray bars) and cross-sectional average (dashed line).

Figure 4 plots the values of $\hat{\Lambda}_{\mathbb{X}}$ and $\hat{\Lambda}_{\mathbb{Y}}$. The 68% credible regions shaded in grey show that factor loadings $\hat{\Lambda}_{\mathbb{X}}$ for temperature are more precisely estimated than the $\hat{\Lambda}_{\mathbb{Y}}$ for GSP growth. Averaged across states, $\hat{\Lambda}_{\mathbb{X}}$ and $\hat{\Lambda}_{\mathbb{Y}}$ are both around one. However, $\hat{\Lambda}_{\mathbb{X}}$ has a cross-sectional standard deviation of 0.226, much smaller than the 0.472 obtained for $\hat{\Lambda}_{\mathbb{Y}}$. It is interesting that $\hat{\Lambda}_{\mathbb{X}}$ is large for the states along the coast and smaller for states inland, while $\hat{\Lambda}_{\mathbb{Y}}$ is larger in the East Coast than the West Coast. This observation is corroborated by a heatmap of R^2 from a regression of \mathbb{X}_i on its common component $\hat{\Lambda}'_{\mathbb{X}i}\hat{F}$ (not shown), suggesting that idiosyncratic variations dominate the common variations for states inland. Also, consistent with Figure 1, states that have large changes in the low-frequency component over time are also the ones with a dominating common component. The results suggest

common, idiosyncratic, high- and low-frequency variations in X_i and ΔY_i with quite a bit of heterogeneity across states.

Figure 5 presents a common-idiosyncratic view of the aggregate data. The left panel plots the deviation of aggregate GSP growth from its mean (in black dots), the low-frequency component of aggregate GSP growth estimated by MW4 (in blue), and a decomposition of the low-frequency component into a common (in red) and idiosyncratic (in brown bars) component using the framework of Foerster et al. (2022)). Evidently, the idiosyncratic component of growth aligns with recessions in 1975, 1982, 2008, and 2020, while the low-frequency component moves closely with the common component. The right panel of Figure 5 plots the same components for the national temperature series. Many of the spikes in the temperature data coincide with the idiosyncratic component, while the low-frequency component aligns with the common component. The eye-catching feature in Figure 5 is the wavy downward trend in $\hat{\mathcal{L}}_{AY}$ (left panel) and the stark upward trend in $\hat{\mathcal{L}}_{AX}$ (right panel).¹¹ The next section considers if this apparent negative relationship is statistically significant using regressions.

Figure 5: Aggregate Variations by Components for the U.S.



This figure presents the deviation from mean of v (a black dashed line), as well as the low-frequency component of v estimated using MW4 (in blue), its decomposition into a common component (in red) and idiosyncratic error (in brown bars) using the framework of Foerster et al. (2022)). The variable v is aggregate output growth ΔY (left) and aggregate temperature X (right).

¹¹It is also worth noting that the Durbin-Watson statistic from regressions of the log level of GDP on temperature is small, suggesting that the relation might be spurious.

3 Estimating the Economic Impact of Warming Temperature

There is a large body of work studying the impact of environmental changes on the economy. See Dell et al. (2014) for a review of the methodologies used. Most recent econometric analyses are based on static panel regressions and have two notable features. First, they estimate the effects of X , a long difference of X , or ΔX on ΔY . Tol (2024) reviews recent estimates and finds that while the impact of warming is generally found to be negative, there are considerable differences in the magnitude of these estimates, in particular between those with X and those with ΔX as regressors. This is to be expected as zero-frequency variations are removed from the latter, while the former maintains a strong low-frequency component. Second, most econometric analyses control for individual or year effects in an additive way.

A different body of work such as, Bilal and Kanzig (2024) and Nath et al. (2024), use local projections to trace out the dynamic effects of shocks to X , which can be quite different from shocks to \mathcal{L}_X^0 or \mathcal{H}_X^0 . Concerned about the use of year effects in these regressions, Berg et al. (2024) analyze international data using a common-idiosyncratic decomposition of X . Our focus is on a decomposition of the components of X rather than a decomposition of X itself.

Instead of X and/or ΔX , we use $\hat{\mathcal{L}}_X$ and $\hat{\mathcal{H}}_X$ as regressors. Many regressions considered in the literature can be seen as choosing different measures of $\hat{\mathcal{L}}_X$ and $\hat{\mathcal{H}}_X$. For example, ΔX and the number of heating-degree days can be interpreted as a measure of $\hat{\mathcal{H}}_X$. Deviations from a 30-year rolling mean in Kahn et al. (2021) can be similarly be interpreted as $\hat{\mathcal{H}}_X$, with a corresponding $\hat{\mathcal{L}}_X$ that puts an equal weight on each observation in the past 30 years. The mean and deviations from mean in Bento et al. (2023) correspond to using the full sample mean as $\hat{\mathcal{L}}_X$. Bastien-Olvera et al. (2022) employ a low-pass filter with different cutoffs to approximate \mathcal{L}_X^0 , which is similar in spirit to our analysis. As discussed in Mueller and Watson (2008), their cosine transforms produce nearly ideal low-frequency realizations.

3.1 The Regression Framework

Suppose that we have national data, or data for a single country or state. An infeasible regression to learn about the long-run effect of \mathcal{L}_X^0 on ΔY is

$$\Delta Y_t = \beta_0 + \beta_{\mathcal{L}} \mathcal{L}_{X,t}^0 + u_{Y,t}^0.$$

If the low-frequency component \mathcal{L}_X^0 is $I(1)$ and u_Y^0 is stationary, the above regression would consistently estimate the cointegrating relation between the two variables. We only assume

that \mathcal{L}_X^0 have non-trivial variations at frequency close to zero, but do not require d to be integer valued. The feasible regression replaces \mathcal{L}_X^0 with an estimate $\hat{\mathcal{L}}_X$,

$$\Delta Y_t = \beta_0 + \beta_{\mathcal{L}} \hat{\mathcal{L}}_{X,t} + u_{Y,t}. \quad (1)$$

Note that \mathcal{H}_X^0 is consolidated into the error term u_Y^0 in this model, as its variations are, asymptotically, of lower order than \mathcal{L}_X^0 . However, because the MW estimates $\hat{\mathcal{L}}_X$ and $\hat{\mathcal{H}}_X$ are orthogonal by construction, including $\hat{\mathcal{H}}_X$ in (1) does not affect the estimate of $\beta_{\mathcal{L}}$, but can improve efficiency.

The model for a single unit motivates our panel regressions

$$\Delta Y_{it} = m_{it} + \beta_{\mathcal{L}} \hat{\mathcal{L}}_{X,it} + u_{Y,it}, \quad (2)$$

with different controls for unobserved heterogeneity m_{it} . We consider three specifications:

- i. Model FE: $m_{it} = \gamma_i$;
- ii. Model AFE: $m_{it} = \gamma_i + \xi_t$;
- iii. Model IFE: $m_{it} = \gamma_i + \lambda_i F_t$.

Model FE only controls for unit fixed effects, which would be appropriate if there were no common year effects. Comparing these estimates with model AFE, which also controls for year effects can help gauge the importance of ξ_t . Applied work often uses one-way clustered standard errors (1 way SE) for inference, where clustering is only performed at the unit level. However, as discussed in Majerovitz and Sastry (2023), one-way clustering may not sufficiently characterize all sources of heterogeneity, in particular in the time dimension. Our simulation results in Appendix C illustrate this concern. Specifically, we find that if the common year effect is omitted or affects the states in a non-uniform way, one-way clustered standard errors tend to understate the estimation uncertainty and lead to severe over-rejections of the null hypothesis (up to 80% at 10% nominal levels). In such cases, valid inference in FE and AFE requires two-way clustering in order to account for strong time effects that do not affect the states uniformly. We use the two-way clustered standard errors (2way SE) based on Cameron et al. (2011).

An alternative to correcting the standard errors for correlations in the units temporally and cross-sectionally is to model the correlation directly using an interactive fixed effects (IFE) specification. In this specification, λ_i is an r -vector of factor loadings and F_t is an r -vector of common factors. In our analysis, we set $r = 1$. The estimation is performed using

the iterative procedure suggested by Bai (2009). In this model, the time effects are no longer a simple cross-sectional average at each t (as in model AFE), but are determined by principal component analysis. To account for the relatively small sample used to estimate the latent factor structure, we use a new bootstrap method that preserves the complex dependence structure in the data. For the IFE estimates, we report the 90% and 68% bootstrap-based (fixed-design, percentile bootstrap) confidence intervals, which account for the uncertainty from estimating the latent factor structure.

The parameter $\beta_{\mathcal{L}}$ in the panel regression given by (2) measures the average long-run impact of $\hat{\mathcal{L}}_{X,it}$ (see Phillips and Moon (1999)). To estimate the short-run effects, we use an autoregressive distributed lag model with the same specifications for m_{it} noted above,

$$\Delta Y_{it} = m_{it} + \alpha \Delta Y_{i,t-1} + b_{\mathcal{L}} \hat{\mathcal{L}}_{X,it} + \delta_{\mathcal{H}} \Delta \hat{\mathcal{H}}_{X,it} + \gamma_{\mathcal{H}} \hat{\mathcal{H}}_{X,i,t-1} + u_{Y,it}. \quad (3)$$

The parameters $\gamma_{\mathcal{H}}$ and $\delta_{\mathcal{H}}$ measure the sum and impact of the high-frequency components on economic growth, respectively. By including $\Delta Y_{i,t-1}$, the dynamic regression not only controls for feedback, but also guards against the bias discussed in Klosin (2024).¹² The quantity $\frac{\hat{b}_{\mathcal{L}}}{1-\alpha}$ estimates a long-run effect of a change in $\hat{\mathcal{L}}_X$, assuming $\hat{\mathcal{L}}_X$ is fixed after the change. As the long-run effect depends on the dynamics of $\hat{\mathcal{L}}_{X,it}$, and these are left unmodeled, the parameters of the dynamic regression are not enough to fully determine the long-run effect. However, the static model given in (2) provides a direct estimate of the long-run effect.

3.2 Estimates for U.S. State Panel

In this subsection, we present empirical results based on a panel of U.S. state level data for the 1963–2023 sample using the estimated MWq components of state temperature X_{it} .¹³ To interpret the estimates, note that X_{it} and its components are in degrees Fahrenheit while ΔY_{it} is a growth rate in percent per year. Table 2 presents results for the parameters of interest: $\beta_{\mathcal{L}}$ from the static specification, and $b_{\mathcal{L}}$, $\delta_{\mathcal{H}}$, $\gamma_{\mathcal{H}}$ and α for the dynamic specification.

For model FE, $\beta_{\mathcal{L}}$ and $b_{\mathcal{L}}$ are estimated to be -0.515 and -0.446 , respectively. In contrast, the impact effect associated with $\mathcal{H}_{X,it}$ is only -0.060 . The one-way clustered standard errors (1way SE) – clustered at the state level – are quite small and imply highly

¹²Because $\Delta \hat{\mathcal{L}}_{X,it}$ is small in this data, $\hat{\mathcal{L}}_{X,it-1}$ is highly correlated with $\hat{\mathcal{L}}_{X,it}$, and is therefore omitted from the regression.

¹³The reported results are for a tuning parameter $q = 4$ which ensures similar periodicity (around 30 years) to the one considered for the longer sample. Similar results are obtained for $q = 8$ and 12 . Alternatively, we could estimate the two latent components using the conventional state-space model or the Hartl (2023) method. The results are qualitatively similar and are available from the authors upon request.

Table 2: U.S. Panel Data Regressions

	static	dynamic			
	$\beta_{\mathcal{L}}$	$b_{\mathcal{L}}$	$\delta_{\mathcal{H}}$	$\gamma_{\mathcal{H}}$	α
FE					
estimate	−0.515	−0.446	−0.060	−0.079	0.122
1way SE	(0.051)	(0.053)	(0.038)	(0.051)	(0.029)
2way SE	(0.327)	(0.312)	(0.153)	(0.259)	(0.087)
90% CI	[−1.013, −0.087]	[−0.936, −0.012]	[−0.356, 0.248]	[−0.515, 0.367]	[0.007, 0.234]
68% CI	[−0.814, −0.258]	[−0.743, −0.198]	[−0.239, 0.136]	[−0.342, 0.190]	[0.053, 0.190]
AFE					
estimate	0.360	0.294	−0.089	−0.052	0.127
1way SE	(0.243)	(0.203)	(0.045)	(0.083)	(0.032)
2way SE	(0.285)	(0.259)	(0.064)	(0.124)	(0.045)
90% CI	[−0.228, 0.940]	[−0.272, 0.870]	[−0.255, 0.070]	[−0.264, 0.158]	[0.062, 0.192]
68% CI	[0.003, 0.712]	[−0.048, 0.638]	[−0.185, 0.006]	[−0.185, 0.078]	[0.087, 0.169]
IFE					
estimate	−0.006	−0.062	−0.145	−0.098	0.164
90% CI	[−0.469, 0.414]	[−0.519, 0.342]	[−0.295, 0.010]	[−0.323, 0.124]	[0.099, 0.226]
68% CI	[−0.266, 0.254]	[−0.318, 0.191]	[−0.233, −0.052]	[−0.225, 0.023]	[0.124, 0.203]

The table reports panel regression results for the model with individual fixed effects only (FE, top panel), additive fixed effects with both individual and time effects (AFE, middle panel) and interactive fixed effects with country fixed effects (IFE, bottom panel). Results are presented for the static model (left) and the dynamic specification from Section 3.1 (right). For the FE and AFE models, the table presents point estimates, one-way cluster-robust standard errors (1way SE), two-way cluster-robust standard errors (2way SE), and 90% and 68% bootstrap confidence intervals. For the IFE model, the table presents the estimates, 68% and 90% bootstrap confidence intervals.

significant estimates. The more robust two-way clustered standard errors (2way SE) are several orders of magnitude larger, to the point of eliminating any statistical significance of $\hat{\beta}_{\mathcal{L}}$ and $\hat{b}_{\mathcal{L}}$ at 10% significance levels. To more accurately approximate the various sources of uncertainty associated with these estimates, we also construct and report 68% and 90% (fixed-design) bootstrap confidence intervals for all estimates. The bootstrap confidence intervals lend support to the possibility that the estimated negative effect of $\mathcal{L}_{X,it}$ on ΔY_{it} is statistically significant in model FE.

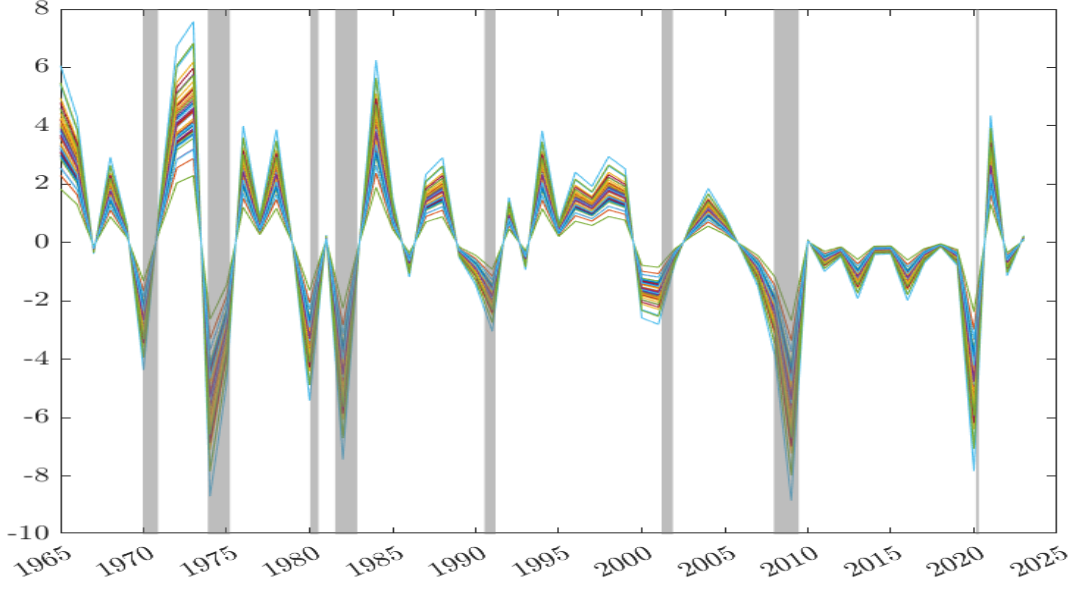
The estimates of $\beta_{\mathcal{L}}$ and $b_{\mathcal{L}}$ for model AFE change sign relative to the FE estimates, suggesting that common time variations have been omitted from model FE. However, model AFE model assumes a homogeneous response to the common year variations, which may be a restrictive assumption. The bottom panel of Table 2 reports estimates from model IFE. Although $\hat{\beta}_{\mathcal{L}}$ and $\hat{b}_{\mathcal{L}}$ in this IFE model are still negative, they are statistically insignificant. Since the coefficient β_X in a regression of ΔY on X is a combination of $\beta_{\mathcal{L}}$ and $\beta_{\mathcal{H}}$, our results suggest that if we had performed an AFE or IFE regression with X as the regressor, $\hat{\beta}_X$ would also be small and insignificant. Indeed, $\hat{\beta}_X$ from the two regressions are -0.062 and -0.110 respectively. Though negative, the standard errors and confidence intervals all suggest that β_X is not statistically different from zero.

One interesting result that emerges from Table 2 is that the impact effect of $\mathcal{H}_{X,it}$ in the IFE model is estimated to be -0.145 and marginally significant with a 68% bootstrap confidence interval of $[-0.233, -0.052]$. Although -0.145 may seem small, the estimated economic magnitude can be large because the high-frequency component $\mathcal{H}_{X,it}$ is more variable than its low-frequency counterpart $\mathcal{L}_{X,it}$. Overall, the relationship between temperature and economic activity in the U.S. panel – to the extent there is one – is more likely to be driven by high-frequency weather variations such as heat waves or natural disasters.

To better understand why standard errors are sensitive to the type of clustering, Figure 6 plots the estimated interactive fixed effect for all 48 states implied by model IFE. As the troughs coincide with recession dates, it is clear that $\hat{F}\hat{\lambda}'$ is picking up business cycle conditions. Given that F_t is common at each t , the heterogeneity shown in $\hat{\lambda}_i$ is inconsistent with the assumption of a common response to F_t underlying model AFE. Thus, the residuals of the additive fixed effect specifications remain correlated and necessitate two-way clustering in the construction of the standard errors. The inclusion of these effects in model IFE helps control for high-frequency variations in GSP growth, making it easier to detect a low-frequency relationship with $\hat{\mathcal{L}}_X$.

Finally, to assess the finite-sample properties of the estimators and the inference proce-

Figure 6: Plot of $\hat{F}\hat{\lambda}'$ in Model IFE



Shaded areas signify NBER recessions.

dures used in this section, Appendix C (Tables C1 and C2) reports Monte Carlo simulation evidence from a model that is calibrated to U.S. data. Despite the relatively small time-series and cross-sectional dimensions, the estimators are relatively well centered around their true values and the bootstrap confidence intervals have reliable coverage rates.

3.3 International Panel

Our choice of a U.S. panel was primarily driven by uniformity in the quality of economic data, as well as the large geographical variation in climates across U.S. states. However, the pronounced factor structure that characterizes unobserved heterogeneity may be specific to U.S. data. To collect further evidence, we also consider an international panel of real GDP growth and temperature as described in Appendix A. The quality of economic data again drives our decision to select only the top 50 countries from the Data Quality Ratings produced by World Economics. In addition to aligning the quality of the economic data, these countries span all continents, which better captures global climate changes over the sample. The main limitation of these data is that economic growth is not available for the recent past, 2019 to 2024. Temperatures are reported in Celsius, and X_i are defined as deviations from their pre-1980 mean.

We first focus on 20 European countries that are a subset of the larger international panel. As in the U.S., there are significant spatial variations in the European data. The Nordic countries (e.g., Denmark, Finland, Norway, Sweden) tend to exhibit larger volatility in X than those in Southern Europe (e.g., Italy, Greece, Spain, Portugal). While $\hat{\mathcal{L}}_{X,i}$ is quite flat in Ireland and Great Britain, there is a notable upward trend in $\hat{\mathcal{L}}_{X,i}$ for Austria, France, Germany, and Italy. More generally, low-frequency variations seem to be stronger in Europe than in the U.S.

Table 3 summarizes the European data in terms of the UC parameters estimated over the full sample, 1901-2022 with $\sigma_{\mathcal{L}} = 0.2$. The countries whose $\hat{\mathcal{L}}_X$ experienced the smallest change over this period are Ireland, Great Britain, Greece, and Israel, while the countries with the largest changes are Austria, Switzerland, Luxembourg, and France. The innovations to the high-frequency component are largest in the Scandinavian countries and smallest in Malta, Portugal, and Spain.

Since, the UC and MWq estimates of \mathcal{L}_X are similar, we proceed with a common-idiosyncratic decomposition based on the latter. The low-frequency estimates also reveal a strong common component. Appendix B presents a decomposition of the variations for aggregate temperature and output growth for the 1953–2018 sample, analogous to Figure 5 for the U.S. Unlike Figure 5, the negative relation between the $\hat{\mathcal{L}}_Y$ and $\hat{\mathcal{L}}_X$ can also be seen in the pre-1980 sample.

Table 3: UC Estimates for 20 European Countries Ordered by $\sqrt{\hat{\nu}} = \hat{\sigma}_{\mathcal{H}}/\sigma_{\mathcal{L}}$

1901-2022				$T = 122$			
				$\sigma_{\mathcal{L}} = 0.2$			
country	\hat{d}	$\Delta^h \hat{\mathcal{L}}_X$	$\hat{\sigma}_{\mathcal{H}}$	country	\hat{d}	$\Delta^h \hat{\mathcal{L}}_X$	$\hat{\sigma}_{\mathcal{H}}$
Bottom half				Top half			
MLT	1.367	1.745	0.307	CHE	1.386	2.114	0.511
PRT	1.383	1.679	0.320	AUT	1.347	2.103	0.549
ESP	1.382	1.902	0.326	LUX	1.354	1.917	0.570
ITA	1.364	1.853	0.363	BEL	1.343	1.732	0.576
IRL	1.124	0.698	0.375	NLD	1.326	1.634	0.591
GRC	1.345	1.270	0.397	DEU	1.332	1.853	0.597
GBR	1.228	1.217	0.434	DNK	1.293	1.537	0.728
CYP	1.424	1.649	0.472	NOR	1.268	1.292	0.742
FRA	1.357	1.885	0.477	SWE	1.290	1.423	0.802
ISL	1.499	1.104	0.493	FIN	1.333	1.654	0.946

X is deviation from the pre-1980 mean. $\Delta^h \hat{\mathcal{L}}_X = \hat{\mathcal{L}}_{X,2021} - \hat{\mathcal{L}}_{X,1901}$, \mathcal{L}_X estimated by the UC model with $\sigma_{\mathcal{L}} = 0.2$, \hat{d} is the long memory parameter, $\hat{\sigma}_{\mathcal{H}}$ is the innovation to the high-frequency component.

Table 4, which presents results for the panel data regression results, follows the same format as Table 2, with the first two panels presenting the results for the two specifications of additive fixed effects and the bottom panel presenting results for the interactive fixed effects model. The main finding is that the estimates of $\beta_{\mathcal{L}}$ and $b_{\mathcal{L}}$ are much larger in magnitude than the ones for the U.S panel and are highly statistically significant. For example, the estimates of $\beta_{\mathcal{L}}$ and $b_{\mathcal{L}}$ in the FE specification are -1.558 and -1.066 , respectively. In the static IFE model, $\hat{\mathcal{L}}_X$ is estimated to have an effect of -0.947 , with a 90% bootstrap confidence interval of $[-1.565, -0.328]$. In the dynamic specification, the point estimate of $b_{\mathcal{L}}$ is -0.808 , with a 90% bootstrap confidence interval of $[-1.392, -0.211]$. The cross-sectional average of $\hat{\mathcal{L}}_X$ in Europe rose by 1.461°C between 1980 and 2018, suggesting a loss in European GDP growth of more than 1.3 percentage points over this period. The first-order effect of $\hat{\mathcal{H}}_X$ is not significant though, as the point estimate of $\gamma_{\mathcal{H}}$ is -0.194 with a 68% bootstrap confidence interval of $[-0.505, 0.098]$. Finally, the estimated coefficient on the lagged dependent variable in the dynamic specification, α , suggests a higher persistence of GDP growth in the European panel than the U.S. state panel.

The panel regression results for the larger international panel ($N = 50$) are reported in Table 5. Consistent with the European panel, the results point to a fairly large negative and statistically significant effect of the low-frequency component of temperature on economic activity. For the FE model, $\hat{\beta}_{\mathcal{L}}$ and $\hat{b}_{\mathcal{L}}$ are -0.911 and -0.659 , respectively. The differences between the one-way and two-way clustered standard errors are now smaller, reflecting a larger idiosyncratic variation across countries. Nevertheless, the one-way clustered standard errors continue to understate the underlying estimation uncertainty. Both 90% and 68% bootstrap confidence intervals indicate statistical significance for the estimates of both $\beta_{\mathcal{L}}$ and $b_{\mathcal{L}}$. In our preferred IFE specification, the effect of the low-frequency component is estimated to be -1.401 with a 90% bootstrap confidence interval $[-2.002, -0.743]$. In the absence of further mitigation policies, an additional 1°C rise in $\hat{\mathcal{L}}_X$ would shave off GDP growth by 1.40 percentage points over the period of this low-frequency temperature increase.

Taken together, the results from the European and international panels provide convincing evidence on the differential effects of the low- and high-frequency components of temperature on real GDP growth, reaffirming the importance of accurately characterizing low-frequency temperature movements in assessing their effects on economic activity.

Table 4: European Panel Data Regressions

	static	dynamic			
	$\beta_{\mathcal{L}}$	$b_{\mathcal{L}}$	$\delta_{\mathcal{H}}$	$\gamma_{\mathcal{H}}$	α
FE					
estimate	−1.558	−1.066	0.073	−0.194	0.318
1way SE	(0.186)	(0.178)	(0.128)	(0.136)	(0.063)
2way SE	(0.392)	(0.390)	(0.248)	(0.303)	(0.079)
90% CI	[−2.133, −0.979]	[−1.605, −0.543]	[−0.320, 0.469]	[−0.745, 0.349]	[0.241, 0.398]
68% CI	[−1.921, −1.215]	[−1.404, −0.746]	[−0.162, 0.317]	[−0.516, 0.133]	[0.272, 0.365]
AFE					
estimate	−0.431	−0.339	0.194	−0.051	0.274
1way SE	(0.927)	(0.670)	(0.271)	(0.271)	(0.043)
2way SE	(0.946)	(0.691)	(0.312)	(0.338)	(0.044)
90% CI	[−1.484, 0.629]	[−1.373, 0.665]	[−0.235, 0.610]	[−0.610, 0.467]	[0.201, 0.345]
68% CI	[−1.097, 0.166]	[−0.930, 0.243]	[−0.054, 0.446]	[−0.393, 0.261]	[0.231, 0.320]
IFE					
estimate	−0.947	−0.808	0.150	−0.194	0.345
90% CI	[−1.565, −0.328]	[−1.392, −0.211]	[−0.234, 0.550]	[−0.731, 0.337]	[0.277, 0.415]
68% CI	[−1.309, −0.570]	[−1.134, −0.451]	[−0.084, 0.369]	[−0.505, 0.098]	[0.303, 0.383]

See notes to Table 2.

Table 5: International Panel Data Regressions

	static	dynamic			
	$\beta_{\mathcal{L}}$	$b_{\mathcal{L}}$	$\delta_{\mathcal{H}}$	$\gamma_{\mathcal{H}}$	α
FE					
estimate	−0.911	−0.659	0.125	−0.185	0.274
1way SE	(0.259)	(0.196)	(0.134)	(0.111)	(0.039)
2way SE	(0.430)	(0.395)	(0.237)	(0.310)	(0.060)
90% CI	[−1.542, −0.303]	[−1.238, −0.088]	[−0.258, 0.493]	[−0.714, 0.355]	[0.223, 0.329]
68% CI	[−1.303, −0.557]	[−1.015, −0.345]	[−0.110, 0.364]	[−0.516, 0.130]	[0.244, 0.307]
AFE					
estimate	−0.009	−0.014	0.284	0.131	0.259
1way SE	(0.681)	(0.508)	(0.139)	(0.153)	(0.041)
2way SE	(0.750)	(0.578)	(0.187)	(0.223)	(0.060)
90% CI	[−0.842, 0.766]	[−0.768, 0.663]	[−0.021, 0.595]	[−0.303, 0.537]	[0.211, 0.306]
68% CI	[−0.528, 0.452]	[−0.477, 0.401]	[0.092, 0.477]	[−0.130, 0.382]	[0.231, 0.291]
IFE					
estimate	−1.401	−0.822	−0.013	0.183	0.251
90% CI	[−2.002, −0.743]	[−1.422, −0.215]	[−0.325, 0.268]	[−0.234, 0.579]	[0.196, 0.300]
68% CI	[−1.766, −1.024]	[−1.172, −0.436]	[−0.210, 0.159]	[−0.073, 0.421]	[0.216, 0.281]

See notes to Table 2.

3.4 Additional Evidence on Heterogeneity and Nonlinearity

The results regarding the average relationship between temperature and economic activity in the previous section are based on panel data regressions. In this section, we consider time series estimates at the aggregate level, as well as an aggregate of state level and country level time series estimates. Lastly, the potential for nonlinear effects is considered.

In Section 2, we find that the national estimate of \mathcal{L}_X^0 is similar to the aggregate of the state level estimates $\mathcal{L}_{X,i}^0$. An alternative to panel data regressions, therefore, is to use national data to estimate the time series regression shown in (1). Because there is only one entity, there is no need to deal with heterogeneity across units. Using national data for the U.S., we obtain an estimate of -0.366 for $\beta_{\mathcal{L}}$. Given that $\hat{\mathcal{L}}_X$ increased by 3.046°F in the estimation sample, the point estimate of the economic loss is meaningful.¹⁴ However, the estimate has large sampling uncertainty, with a 90% confidence interval of $[-0.818, 0.086]$. Thus, similar to panel estimates, the long-run effect of $\hat{\mathcal{L}}_X$ on ΔY is not statistically different from zero in the U.S. data.¹⁵

The pooled estimate from the panel regression (2) could mask the heterogeneity of the economic impact across units. Thus, we also estimate time-series regressions of ΔY_i on $\hat{\mathcal{L}}_{X,i}$ and $\hat{\mathcal{H}}_{X,i}$ for each unit i in the panel under consideration. The left chart in Figure 7 plots the density of the U.S. state-level estimates for $\beta_{\mathcal{L},i}$. While the dispersion in $\beta_{\mathcal{L},i}$ estimates is large, most of the probability mass lies in the negative region. The median of the $\beta_{\mathcal{L},i}$ estimates is -0.584 , with the mode of the density at -0.587 . The population-weighted mean of $\hat{\beta}_{\mathcal{L}}$ for the U.S. is -0.384 (dashed red line in Figure 7), which is very similar to the estimate from national data of -0.366 reported above (solid red line in Figure 7).

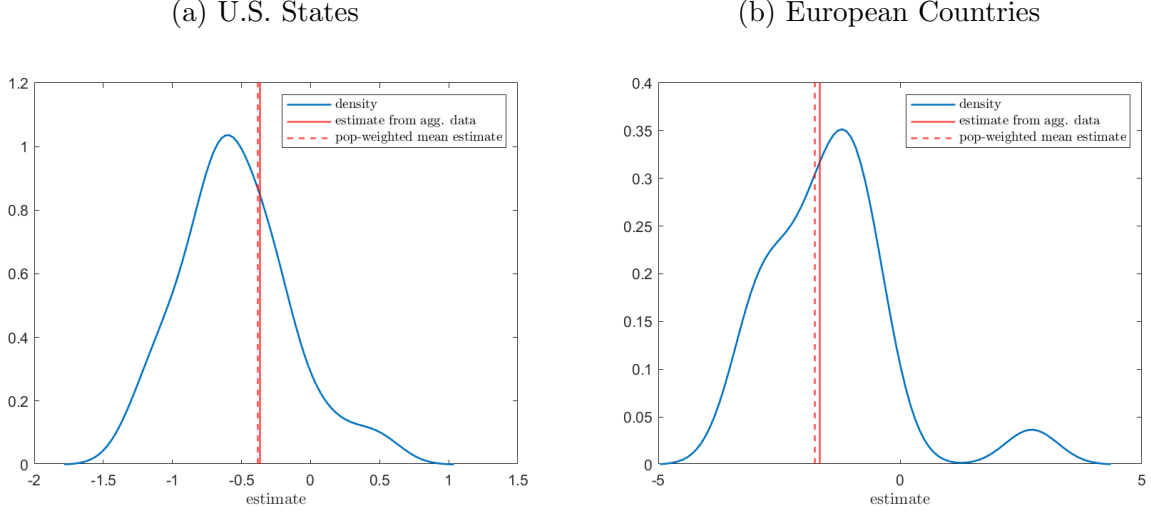
The right panel of Figure 7 presents a density plot of the estimates of $\beta_{\mathcal{L},i}$ from the European sample. Compared U.S. (left), this density is significantly more dispersed. Except for one positive value – Ireland – all remaining point estimates are negative.¹⁶ Ten of the negative estimates are statistically significant at 5% nominal levels, with Newey-West t -statistics between -2.341 and -5.301 . The mass of the density is concentrated deeper in the negative range, and the negative values are larger in absolute magnitude than those for the

¹⁴A time series regression of national ΔY on national X gives an estimate of -0.302 with a 90% confidence interval is $[-0.609, 0.005]$.

¹⁵It is easy to show that the OLS estimate from a regression of ΔY on $\hat{\mathcal{L}}_X$ is numerically identical to the one from a regression of $\hat{\mathcal{L}}_Y$ on $\hat{\mathcal{L}}_X$ so that this could be interpreted as a cointegrating model. One possible way to correct for the potential endogeneity bias in this setting is to employ a dynamic OLS (DOLS) regression. Given the smoothness of $\hat{\mathcal{L}}_X$, however, introducing additional leads and lags of $\Delta \hat{\mathcal{L}}_X$ results in very wide confidence intervals for $\beta_{\mathcal{L}}$ due to potential collinearity.

¹⁶Dropping Ireland increases the pooled IFE estimate from -0.947 to -1.013 .

Figure 7: Density of OLS estimates of $\beta_{\mathcal{L}}$



This figure plots the density of $\beta_{\mathcal{L}}$ from state-by-state (48 U.S. states, left chart) and country-by-country (20 European countries, right chart) time series regressions. The two charts also present the OLS estimate of $\beta_{\mathcal{L}}$ from the U.S. and European aggregate regressions (solid red line), along with the population-weighted mean of the individual estimates (dashed red line).

U.S. The mode of the density for $\{\hat{\beta}_{\mathcal{L},i}\}$ in Europe is -1.198 and the median is -1.458 , with a population-weighted average (dashed red line) of -1.761 . Similar to the U.S. analysis, we construct population-weighted aggregate data for these 20 European countries and estimate $\beta_{\mathcal{L}}$ from a time-series regression using this aggregated data. The OLS estimate of $\beta_{\mathcal{L}}$ from this regression is -1.662 (solid red line in the right chart) with a 90% confidence interval of $[-2.322, -1.002]$. This estimate is larger than the pooled estimate of -0.947 reported earlier, very close to the population weighted average, and is statistically different from zero.

As surveyed in Hsiang (2016), many studies have found non-linear relationships between temperature and economic outcomes when (time-invariant) summary statistics of climate across space are interacted with temperature. Kalkuhl and Wenz (2020) interact X_t with ΔX_t . In the same spirit, we introduce $\hat{\mathcal{H}}_{X,it} \times \hat{\mathcal{L}}_{X,it}$ as an additional (time-varying) regressor in the static specification of our preferred interactive fixed effects model. This allows for the possibility of a new form of nonlinearity via an interaction term of the low- and high-frequency components with a corresponding coefficient $\beta_{\mathcal{H}\mathcal{L}}$. The marginal effect of $\hat{\mathcal{H}}_X$ on ΔY is computed as $\hat{\beta}_{\mathcal{H}} + \hat{\beta}_{\mathcal{H}\mathcal{L}}\bar{\mathcal{L}}_{X,t}$, where $\bar{\mathcal{L}}_{X,t}$ is the cross-sectional average of $\hat{\mathcal{L}}_{X,it}$. The marginal effect of $\hat{\mathcal{L}}_X$ on ΔY is similarly computed as $\hat{\beta}_{\mathcal{L}} + \hat{\beta}_{\mathcal{H}\mathcal{L}}\bar{\mathcal{H}}_{X,t}$.

Table 6 presents estimates and bootstrap confidence intervals from this nonlinear specification for the U.S. (top), European (middle) and international (bottom) panels. Compared

Table 6: Results from Nonlinear Panel Data Regressions

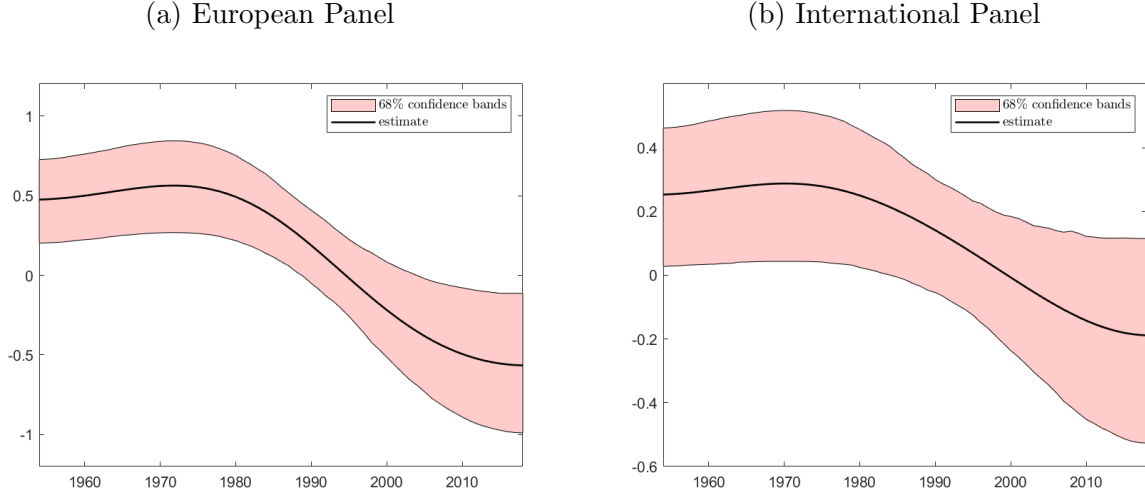
	$\beta_{\mathcal{L}}$	$\beta_{\mathcal{H}}$	$\beta_{\mathcal{H}\mathcal{L}}$
U.S. estimate	−0.002	−0.046	−0.072
90% CI	[−0.466, 0.419]	[−0.256, 0.158]	[−0.209, 0.064]
68% CI	[−0.263, 0.258]	[−0.166, 0.085]	[−0.160, 0.010]
European estimate	−0.910	0.540	−0.834
90% CI	[−1.543, −0.286]	[0.029, 1.002]	[−1.524, −0.162]
68% CI	[−1.288, −0.528]	[0.253, 0.815]	[−1.247, −0.387]
International estimate	−1.403	0.300	−0.381
90% CI	[−2.004, −0.739]	[−0.136, 0.705]	[−0.972, 0.201]
68% CI	[−1.769, −1.018]	[0.046, 0.537]	[−0.710, −0.038]

The table reports panel regression results for the static interactive fixed effects model with explanatory variables $\hat{\mathcal{H}}_{it}$, $\hat{\mathcal{L}}_{it}$, and $\hat{\mathcal{H}}_{it} \times \hat{\mathcal{L}}_{it}$. The table presents point estimates, 90% and 68% bootstrap confidence intervals for the U.S. (top), European (middle) and International (bottom) panels.

to the results in Tables 2, 4 and 5, the estimates of $\beta_{\mathcal{L}}$ are largely unchanged and the interaction term does not provide evidence for a nonlinear effect in the low-frequency component. However, in our model, nonlinearity is captured implicitly by the shape of $\hat{\mathcal{L}}_X$ which has an upward trend since 1980. We find that though the estimate of $\beta_{\mathcal{H}\mathcal{L}}$ is also negative, the marginal effect of $\hat{\mathcal{L}}_X$ is actually dampened when evaluated at the cross-sectional average of $\hat{\mathcal{H}}_X$, as this average is close to zero.

By contrast, the effect of the high-frequency component $\hat{\mathcal{H}}_X$ in the European panel – which was close to zero and statistically insignificant in the linear specification – now exhibits pronounced nonlinearity, as $\hat{\beta}_{\mathcal{H}}$ and $\hat{\beta}_{\mathcal{H}\mathcal{L}}$ appear to be significant with opposite signs. The results for $\hat{\mathcal{H}}_X$ in the international panel also suggest some nonlinearity, while this is not the case for the U.S. data. Figure 8 plots the marginal effect of $\hat{\mathcal{H}}_X$ on ΔY defined above for the European and international panels, along with 68% bootstrap confidence bands. While the uncertainty associated with these estimates is large, there is some evidence that the effect of $\hat{\mathcal{H}}_X$ has switched from positive to negative since the 1980s. However, evaluated at any t , the total (linear effect and nonlinear) effect from a change in $\hat{\mathcal{H}}_X$ in both panels is noticeably smaller than the estimate for $\beta_{\mathcal{L}}$, which supports our premise that low- and high-frequency changes in temperature have differential economic impacts.

Figure 8: Estimated effect of $\hat{\mathcal{H}}_{\mathcal{X}}$ on ΔY , evaluated at the cross-sectional average of $\hat{\mathcal{L}}_{\mathcal{X}}$



The estimated marginal effect is in solid black line with 68% bootstrap confidence bands as the shaded area.

4 Concluding Remarks

Since the late 1970s, global temperatures have registered a persistent increase that manifested in a clear break from its pre-1980 mean. In fact, 2024 was the warmest year on record, with global temperatures exceeding the pre-industrial (1850–1900) average by 1.46°C. Our analysis is premised on the fact that year-over-year changes in temperature are comprised of variations with different degrees of persistence, and each can have a distinctive impact on economic activity. In all three panels of data studied, the estimated low-frequency component temperature displays a persistent increase since the 1970s, around the same time as the well-documented slowdown in economic growth. This informal finding guided our choice of a regression model that allows the low- and high-frequency components of temperature to have different economic impacts and heterogeneous responses to business cycle related common variations in estimation and inference. Panel and time series regressions find a negative first-order effect of the low-frequency component of temperature on economic growth that is strong and statistically significant in the international and European panels, but no effect in the U.S. panel. The high-frequency component is estimated to have no first-order effect in the international data, but does exhibit a small non-linear effect through interaction with the low-frequency component that is statistically significant.

Appendix A Data Description

U.S. Panel

Average temperature series for the U.S. panel are from NOAA nClimDiv, natively at the county-month level.¹⁷ These are then (1) spatially averaged to the state level using author-constructed static population weights, and (2) averaged over time to the yearly level. The temperature series are recorded in °F and expressed as deviations from their pre-1980 mean.

Static county population weights are produced by calculating the percent of the total state population represented by each county in the 2020 IPUMS NHGIS population dataset. State population data are obtained from FRED at the yearly level. These population weights are used in computing the population-weighted averages reported in the paper.

Real Gross State Product (GSP) series are obtained from multiple sources. For data after (and including) 1997, our source is the Bureau of Economic Analysis (BEA). As they have deprecated all data before this (both for nominal and real series), we rely on the data used in Mohaddes et al. (2023) as presented in their replication package. They describe appending (1) the deflated nominal GSP by state-level CPI from 1963 to 1976, and (2) the real GSP as provided by the BEA from 1977 to 1996. In order to harmonize the Mohaddes et al. (2023) series with the latest data, we normalize their price base by multiplying their data by the ratio of their 1997 value and the value for 1997 as obtained through the BEA.

Because of missing values, Hawaii, Alaska, and the District of Columbia are dropped, giving us a cross-sectional dimension of $N = 48$. The temperature data are available at the state level from 1895 to 2023 (i.e., $T = 129$). After we merge temperature and real GSP growth data, the sample period is 1964–2023 and $T = 60$.

International Panel

Average temperature series for the international panel are from CRU TS, natively at the 30 minute grid-year level. These are then spatially averaged to the country level using author-constructed static population weights. The temperature series are in °C, and again expressed as deviations from their pre-1980 mean.

Static grid cell population weights are produced by calculating the percent of the total country population represented by each grid cell in the 2020 Gridded Population of the World file. Real Gross Domestic Product (GDP) and country population is obtained from

¹⁷The data are available at the 30 minute (grid)-year level. We merge it with 30 minute population weights in 2020 to obtain spatial averages.

the 2023 Maddison Project Database. These static (as of 2020) population weights are used in computing the population-weighted averages reported in the paper. The temperature data is available for the 1901-2022 period.

To ensure the reliability of GDP and population data, we use the Data Quality Ratings produced by World Economics. Our international panel is comprised of 50 countries with the highest combined ranking in this index. More specifically, we initially use their letter grade for GDP per capita to rank countries and then sort by the minimum of the GDP and population quality index values within these letter grades.

The 50 countries in our international panel are: Switzerland, Canada, Ireland, Australia, Great Britain, Puerto Rico,¹⁸ USA, Japan, New Zealand, France, Singapore, Slovenia, Taiwan, Korea, Denmark, Sweden, Netherlands, Spain, Norway, Portugal, Italy, Germany, Austria, Poland, Finland, Chile, Mauritius, Hungary, Malta, Colombia, North Macedonia, Mongolia, Brazil, Turkey, Malaysia, Philippines, Belgium, Luxembourg, Cyprus, Iceland, Greece, Israel, Romania, Croatia, Bulgaria, UAE, South Africa, Uruguay, Jordan, Morocco. The real GDP data for each country is at an annual frequency for the period 1952–2018. After constructing growth rates for real GDP, the resulting panel is of dimensions $T = 66$ and $N = 50$.

Finally, our European panel is a subset of the international panel and is comprised of 20 European countries with sufficient geographic variation across the European continent (no Eastern European countries are included). These countries (with their corresponding abbreviations in parentheses) are: Switzerland (CHE), Ireland (IRL), Great Britain (GBR), France (FRA), Denmark (DNK), Sweden (SWE), Netherlands (NLD), Spain (ESP), Norway (NOR), Portugal (PRT), Italy (ITA), Germany (DEU), Austria (AUT), Finland (FIN), Malta (MLT), Belgium (BEL), Luxembourg (LUX), Cyprus (CYP), Iceland (ISL), Greece (GRC). For this panel, $T = 66$ and $N = 20$.

¹⁸Puerto Rico is assumed to have the same data quality as the United States.

Appendix B Alternative Estimators of \mathcal{L}^0

The MWq procedure of Mueller and Watson (2008, 2017, 2022) is described in the main text (Section 2.2).

The HP(λ) filter of Hodrick and Prescott (1997) uses a two-sided smoother with parameter λ to approximate the slow-moving component. Phillips and Jin (2021) and Phillips and Shi (2021) show that boosting, or repeated application of the HP-filter can improve trend estimates if the data are integrated of order $d \in [0, 1]$. Specifically, ‘bHP’ produces $\mathcal{L} = Z - \mathcal{H}$, where $\mathcal{H} = (I_n - S(\lambda))^m Z$, $S(\lambda) = (I_T + \lambda D_2 D_2')^{-1}$, D_2' is a $(T - 2) \times T$ submatrix of the $T \times T$ Toeplitz matrix whose first row is $(1, -2, 1, 0_{T-3})$. Without iteration, bHP(λ) is the HP(λ), but the bHP endogenously adjusts λ at each step of the iteration. Building on this work, Biaswas et al. (2023) establish the conditions under which bHP can also be applied to data with long-range dependence.

Hamilton (2018) forcefully argues that the HP filters create spurious dynamics. The proposed JH(h,p) procedure constructs $\mathcal{H}_t = Z_{t+h} - \text{proj}(Z_{t+h} | Z_t, Z_{t-1}, \dots, Z_{t-p})$, which is the unpredicted value of Z_{t+h} based on information at time t and earlier. This amounts to taking $\hat{\mathcal{L}}$ to be the fit from regressing Z_{t+h} on values of Z_t and its p lags. The $\hat{\mathcal{L}}$ produced by JH is a filtered estimate of \mathcal{L}^0 which will be more variable than MWq and bHP because these two are based on two-sided smoothing, and thus subject to ‘look-ahead’ bias.

Finally, Figure B1 presents a decomposition of the variations for temperature and output growth for the 20 European countries.

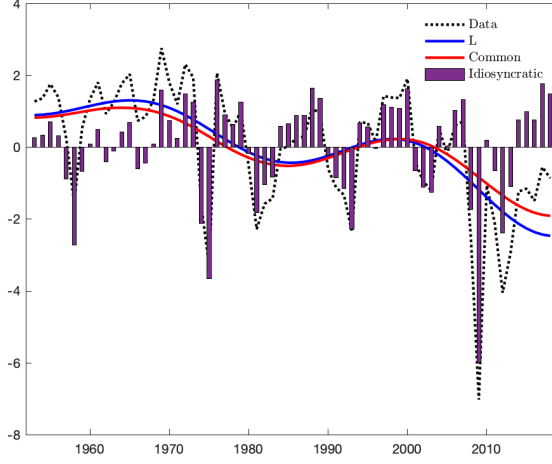
Appendix B.1 A Monte Carlo Exercise for Estimation of \mathcal{L}_X^0

The procedures described in 2 are designed for trending filtering of economic data. We do not know how accurate they are for estimating temperature trends, and for this, we need to know the true underlying low-frequency component which is never observed. We thus design a Monte-Carlo exercise calibrated to several temperature series to evaluate the total (approximation plus sampling) mean-squared error of the procedures.

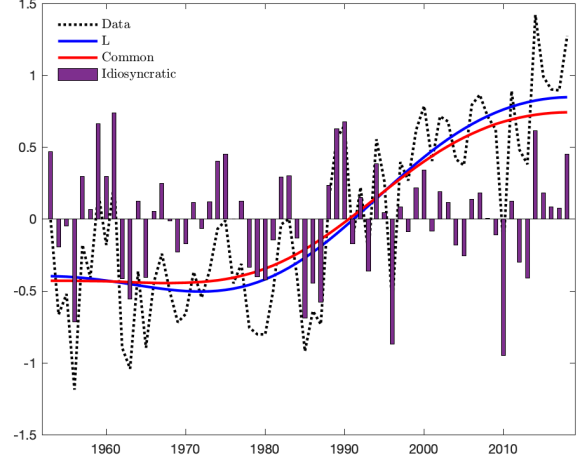
We use the UC model to generate data in the Monte-Carlo exercise, and the parameters for that model are $(d, \sigma_{\mathcal{L}}, \sigma_{\mathcal{H}}, a_1)$. We select the following seven states which have different configurations of $(\hat{d}, \hat{\sigma}_{\mathcal{H}})$: California (CA), Florida (FL), Illinois (IL), Massachusetts (MA), North Dakota (ND), New York (NY), and Washington (WA). As seen from Table 1, ND has the largest $\hat{\sigma}_H$ while CA and FL have some of the smallest. WA and MA have similar $\hat{\sigma}_{\mathcal{H}}$ but different values of \hat{d} . Except for IL and ND, which are located in the interior of the country, the other four states are along the coast. In each of the S simulations of data for state i , \mathcal{L}_{it}^0

Figure B1: Aggregate Variations by Components for Europe

(a) GDP Growth



(b) Temperature



See notes to Figure 5.

is fixed to be $\hat{\mathcal{L}}_{it}$, the state-level estimate with $\sigma_{\mathcal{L}} = 0.2$ or 0.4 . The state-specific parameters $(\hat{a}_{i1}, \hat{\sigma}_{i,\mathcal{H}})$ are then used to generate \mathcal{H}_{it}^s , after which $X_{it}^s = \hat{\mathcal{L}}_{it} + \hat{\mathcal{H}}_{it}^s$ is constructed. The simulated series $\{X_{it}^s\}$ is used by different procedures to estimate $\{\mathcal{L}_{it}^s\}$.

Table B1 reports the in-sample root mean-squared error (RMSE). The top panel gives results for $\sigma_{\mathcal{L}} = 0.2$, which will simulate a smoother \mathcal{L}^0 than when $\sigma_{\mathcal{L}} = 0.4$, shown in the bottom panel. Values for \hat{d} and $\hat{\sigma}_{\mathcal{H}}$ used in the calibration are given in the first row. In both cases, the RMSE is largest for ND which is the state with the largest $\hat{\sigma}_{\mathcal{H}}$, and smallest for FL which has the smallest $\hat{\sigma}_{\mathcal{H}}$. Indeed, comparing results across states, the errors are increasing in $\hat{\sigma}_{\mathcal{H}}$. In the top panel when $\sigma_{\mathcal{L}} = 0.2$, MW8 and HP(100) have the smallest RMSE, while JH(h,p) have the largest errors. In the bottom panel when $\sigma_{\mathcal{L}} = 0.4$, MW8 and HP(100) still have the smallest RMSE in six of the seven cases except CA. In that case, the JH procedure has significantly smaller errors. Though HP(100) performs well, it is unclear how to justify the choice of $\lambda = 100$ because, as noted above, the estimates of d are always smaller than the value of two that is implicit in the HP filter.

Table B1: Monte Carlo: In-Sample MSE for X_i

	CA	FL	IL	MA	ND	NY	WA
DGP: $\sigma_a = 0.2$							
$(d, \sigma_{\mathcal{H}})$	(0.99,0.74)	(1.00,0.72)	(0.88,1.37)	(1.06,1.00)	(0.90,1.77)	(1.02,1.05)	(0.84,0.99)
MW(8)	2.709	2.646	4.571	3.462	6.580	3.466	3.617
MW(12)	2.987	2.745	5.478	3.874	7.875	4.037	4.243
MW(16)	3.298	3.060	6.248	4.280	8.989	4.501	4.818
JH(4,4)	4.681	4.511	5.564	5.927	7.410	6.016	4.663
JH(6,6)	5.193	5.090	5.602	6.304	7.500	6.245	4.597
JH(8,8)	6.023	5.684	5.827	7.203	7.764	7.035	4.787
bHP(6.25)	4.265	3.904	8.199	5.615	11.650	5.924	6.249
HP(100)	2.813	2.614	5.217	3.619	7.504	3.791	4.037
DGP: $\sigma_a = 0.4$							
$(d, \sigma_{\mathcal{H}})$	(0.30,0.80)	(0.76,0.64)	(0.66,1.33)	(0.83,0.94)	(0.71,1.74)	(0.80,1.00)	(0.63,0.93)
MW(8)	11.477	3.494	4.611	3.965	6.505	3.821	3.861
MW(12)	12.682	3.219	5.448	4.051	7.731	4.192	4.214
MW(16)	13.394	3.357	6.144	4.135	8.809	4.384	4.646
JH(4,4)	8.139	4.590	5.633	5.806	7.593	5.909	4.807
JH(6,6)	6.986	5.395	5.705	6.400	7.664	6.323	4.768
JH(8,8)	6.751	5.866	5.932	7.446	7.939	7.228	5.004
bHP(6.25)	14.360	3.414	7.959	5.081	11.383	5.487	5.801
HP(100)	12.120	3.022	5.165	3.646	7.364	3.816	3.972

Reported are results based on 5000 replications. The seven states are California (CA), Florida (FL), Illinois (IL), Massachusetts (MA), North Dakota (ND), New York (NY), and Washington (WA). For each state $i = 1, \dots, 7$ and for each replication s , data $\hat{X}_i^s = \hat{\mathcal{L}}_{X,i} + \hat{\mathcal{H}}_{X,i}^s$ are obtained by generating $\hat{\mathcal{H}}_{X,i}$ using parameter estimates $(\hat{d}, \hat{a}_1, \hat{\sigma}_{\mathcal{H}}^2)$ for state i with $\sigma_{\mathcal{L}}$ held fixed. Results are reported for $\sigma_{\mathcal{L}} = 0.2$ (top panel) and 0.4 (bottom panel).

Appendix C Simulation Evidence for Panel Data Regressions

This section provides simulation evidence for assessing the properties of the estimation and inference methods used in Section 3 of the paper. We consider a dynamic panel data model with (i) interactive fixed effects (IFE) and (ii) individual fixed effects (FE). As in the paper, we are interested in the static and dynamic effects of the low-frequency (\mathcal{L}) and high-frequency (\mathcal{H}) components.

The true processes \mathcal{L}_{it} and \mathcal{H}_{it} are assumed to follow the decomposition described in Section 2.1 for each $i = 1, \dots, N$. The parameters that describe the dynamics of these processes are estimated from the U.S. state temperature data using the Hartl (2023) estimator for $\sigma_{\mathcal{L}} = 0.4, 0.2$, and 0.04. Given the strong factor structure that we documented in the

paper, we postulate that both \mathcal{L}_{it} and \mathcal{H}_{it} are driven by one common factor. We keep the common factor in the state low-frequency components fixed (at their estimated value) in the simulation with variation in the simulated \mathcal{L}_{it} coming only from drawing idiosyncratic errors from a multivariate Gaussian distribution with mean zero and a covariance matrix $\Sigma_{\mathcal{L}}$, calibrated to the data. For the high-frequency common component, we further decompose it into a deterministic component – estimated by MWq with $q = 28$, which is intended to approximate the ENSO cycle – and an AR(1) cyclical component. We keep the deterministic part fixed in simulations and generate AR(1) processes from a Gaussian distribution with AR and variance parameters calibrated to the data. We then build the common factor structure in \mathcal{H}_{it} using the estimated loadings from the data and generate idiosyncratic errors from a multivariate Gaussian distribution with mean zero and variance $\Sigma_{\mathcal{H}}$. All these steps produce simulated data $\tilde{\mathcal{L}}_{it}$ and $\tilde{\mathcal{H}}_{it}$ as well as $\tilde{X}_{it} = \tilde{\mathcal{L}}_{it} + \tilde{\mathcal{H}}_{it}$.

For the FE setup, we generate data for Y_{it} from the model

$$\Delta \tilde{Y}_{it} = \hat{\alpha} \Delta \tilde{Y}_{i,t-1} + \hat{b}_{\mathcal{L}} \tilde{\mathcal{L}}_{it} + \hat{\delta}_{\mathcal{H}} \Delta \tilde{\mathcal{H}}_{it} + \hat{\gamma}_{\mathcal{H}} \tilde{\mathcal{H}}_{i,t-1} + \tilde{u}_{Y,it},$$

where $\tilde{u}_{Y,it} \sim N(0, \hat{\Sigma}_u)$, and $\hat{\alpha}$, $\hat{b}_{\mathcal{L}}$, $\hat{\delta}_{\mathcal{H}}$, $\hat{\gamma}_{\mathcal{H}}$ and $\hat{\Sigma}_u$ are the sample estimates from a dynamic panel data model with individual fixed effects. For the IFE specification, the data for Y_{it} is instead generated from the model

$$\Delta \tilde{Y}_{it} = \hat{\alpha} \Delta \tilde{Y}_{i,t-1} + \hat{b}_{\mathcal{L}} \tilde{\mathcal{L}}_{it} + \hat{\delta}_{\mathcal{H}} \Delta \tilde{\mathcal{H}}_{it} + \hat{\gamma}_{\mathcal{H}} \tilde{\mathcal{H}}_{i,t-1} + \hat{\lambda}_i \hat{F}_t + \tilde{u}_{Y,it},$$

where $\tilde{u}_{Y,it} \sim N(0, \hat{\Sigma}_u)$, and $\hat{\alpha}$, $\hat{b}_{\mathcal{L}}$, $\hat{\delta}_{\mathcal{H}}$, $\hat{\gamma}_{\mathcal{H}}$, $\hat{\lambda}_i$, \hat{F}_t and $\hat{\Sigma}_u$ are now the sample estimates from a dynamic panel data model with interactive fixed effects as in Bai (2009).

In order to preserve the main features of the data, we keep $\hat{\lambda}_i \hat{F}_t$ fixed in the simulations. We also remain agnostic about the fact that $\tilde{\mathcal{L}}_{it}$ and $\tilde{\mathcal{H}}_{it}$ are generated by the Hartl procedure and instead we estimate them using the Mueller and Watson (2008, 2017, 2022) method, MWq, for several values of the tuning parameter q . This allows us to assess the effects of uncertainty about \mathcal{L} and \mathcal{H} on the estimation of the parameters of interest. All of the simulated data is of dimension ($T = 60, N = 48$). All results are based on 1,000 Monte Carlo replications.

In addition to estimation, we also evaluate the coverage properties of several inference procedures. Since N is relatively small, it would be desirable for the inference procedure to account for the uncertainty in estimating F_{it} and λ_{it} . For this reason, and given the complex dependence structure in the IFE model, we use a fixed-design bootstrap where the only source of variation comes from resampling the errors $\tilde{u}_{Y,it}$. We use 399 bootstrap samples

to re-estimate all of the model parameters and construct 90% confidence intervals using the percentile method. We use this bootstrap method in both the FE and the IFE designs.

In the individual fixed effects model, standard errors are routinely produced by clustering at state level. But given the strong factor structure documented in Section 3, valid inference necessitates two-way clustering in order to accommodate the more complex dependence structure in these models. While the IFE model explicitly takes this factor structure into account, the FE model leaves it in the errors and the inference procedure needs to be adjusted to reflect this additional source of heterogeneity. For these reasons, we include in the simulations coverage of 90% confidence intervals (based on standard normal asymptotic approximation) using one-way (within i) cluster-robust standard errors (referred to as “asy1” in the Table C2) and two-way cluster-robust standard errors as in Cameron et al. (2011) (referred to as “asy2” in the Table C2).

The results can be summarized as follows. For the IFE model (Table C1), the estimates exhibit little bias. The coverage rates of the 90% bootstrap confidence intervals are close to the nominal level although they undercover for specifications where the variation in X_{it} is dominated by the high-frequency component and q is relatively large. For the FE model (Table C2), we observe a bigger (downward) bias of the estimates although these are relatively minor given the small N and T dimensions. The most striking result is the severe under-coverage of confidence intervals based on one-way clustered standard errors. The two-way clustering substantially improves the coverage of the 90% asymptotic confidence intervals with the bootstrap method delivering further improvements. In summary, this simulation evidence is supportive and reassuring for the results presented in our empirical analysis.

Table C1: Results for the IFE model

coeff	true	$q = 4$			$q = 8$			$q = 12$		
		estim	sd	boot	estim	sd	boot	estim	sd	boot
$\sigma_{\mathcal{L}} = 0.4$										
$b_{\mathcal{L}}$	-0.151	-0.146	0.176	0.864	-0.130	0.158	0.874	-0.125	0.146	0.865
$\delta_{\mathcal{H}}$	-0.128	-0.132	0.097	0.884	-0.133	0.102	0.879	-0.133	0.108	0.884
$\gamma_{\mathcal{H}}$	-0.066	-0.078	0.146	0.878	-0.081	0.159	0.870	-0.080	0.170	0.869
α	0.164	0.142	0.041	0.877	0.143	0.041	0.877	0.143	0.041	0.878
$\sigma_{\mathcal{L}} = 0.2$										
$b_{\mathcal{L}}$	-0.046	-0.064	0.207	0.868	-0.076	0.183	0.860	-0.082	0.169	0.846
$\delta_{\mathcal{H}}$	-0.149	-0.140	0.098	0.889	-0.140	0.104	0.876	-0.140	0.108	0.885
$\gamma_{\mathcal{H}}$	-0.112	-0.113	0.144	0.893	-0.113	0.157	0.882	-0.113	0.168	0.887
α	0.164	0.141	0.040	0.870	0.142	0.040	0.872	0.142	0.040	0.876
$\sigma_{\mathcal{L}} = 0.04$										
$b_{\mathcal{L}}$	-0.033	-0.051	0.209	0.879	-0.067	0.182	0.857	-0.070	0.161	0.856
$\delta_{\mathcal{H}}$	-0.147	-0.142	0.091	0.891	-0.141	0.097	0.886	-0.142	0.103	0.887
$\gamma_{\mathcal{H}}$	-0.109	-0.103	0.136	0.888	-0.100	0.150	0.878	-0.104	0.161	0.881
α	0.164	0.141	0.040	0.864	0.141	0.040	0.862	0.141	0.040	0.865

The table reports the true value of the parameters (“true”), the corresponding average estimates (“estim”) over 1,000 Monte Carlo simulations, their standard deviations (“sd”) and the coverage rates of 90% bootstrap confidence intervals (“boot”). The results are reported for 3 values of $\sigma_{\mathcal{L}}$ (the standard deviation of the low-frequency component \mathcal{L}) and 3 values of q for the MWq procedure, which is used to estimate the latent \mathcal{L} .

Table C2: Results for the FE model

		$q = 4$					$q = 8$				
coeff	true	estim	sd	asy1	asy2	boot	estim	sd	asy1	asy2	boot
$\sigma_{\mathcal{L}} = 0.4$											
$b_{\mathcal{L}}$	-0.525	-0.455	0.301	0.213	0.844	0.855	-0.422	0.280	0.221	0.831	0.844
$\delta_{\mathcal{H}}$	-0.006	-0.058	0.194	0.295	0.881	0.887	-0.053	0.206	0.305	0.868	0.888
$\gamma_{\mathcal{H}}$	-0.016	-0.078	0.285	0.303	0.861	0.877	-0.071	0.310	0.309	0.858	0.880
α	0.122	0.094	0.068	0.330	0.833	0.874	0.096	0.069	0.338	0.835	0.870
$\sigma_{\mathcal{L}} = 0.2$											
$b_{\mathcal{L}}$	-0.500	-0.429	0.311	0.203	0.837	0.849	-0.397	0.290	0.205	0.833	0.846
$\delta_{\mathcal{H}}$	-0.041	-0.063	0.196	0.315	0.858	0.880	-0.060	0.204	0.316	0.869	0.888
$\gamma_{\mathcal{H}}$	-0.049	-0.073	0.285	0.308	0.865	0.882	-0.069	0.308	0.293	0.863	0.883
α	0.121	0.098	0.072	0.310	0.828	0.861	0.100	0.072	0.328	0.825	0.862
$\sigma_{\mathcal{L}} = 0.04$											
$b_{\mathcal{L}}$	-0.522	-0.458	0.309	0.210	0.835	0.853	-0.418	0.291	0.196	0.813	0.838
$\delta_{\mathcal{H}}$	-0.051	-0.057	0.198	0.279	0.847	0.863	-0.055	0.207	0.309	0.856	0.871
$\gamma_{\mathcal{H}}$	-0.061	-0.064	0.286	0.295	0.850	0.873	-0.064	0.307	0.301	0.853	0.866
α	0.120	0.095	0.070	0.320	0.831	0.854	0.097	0.070	0.321	0.830	0.854

The table reports the true value of the parameters (“true”), the corresponding average estimates (“estim”) over 1,000 Monte Carlo simulations, their standard deviations (“sd”), the coverage rates of 90% confidence intervals based on 2 asymptotic approximations (“asy1” for one-way and “asy2” for two-way cluster-robust standard errors), and the coverage rates of 90% bootstrap confidence intervals (“boot”). The results are reported for 3 values of $\sigma_{\mathcal{L}}$ (the standard deviation of the low-frequency component \mathcal{L}) and 2 values of q for the MWq method, which is used to estimate the latent \mathcal{L} .

References

- Bai, J. 2009, Panel Data Models with Interactive Fixed Effects, *Econometrica* **77:4**, 1229–1279.
- Bastien-Olvera, B. A., Granella, F. and Moore, F. C. 2022, Persistent Effect of Temperature on GDP Identified from Lower Frequency Temperature Variability, *Environmental Research Letters* **17:8**, 084038.
- Bento, A., Miller, N., Mookerjee, M. and Severini, S. 2023, A Unifying Approach to Measuring Climate Change Impacts and Adaptation, *Journal of Environmental Economics and Management* **121**, 102834.
- Berg, K., Curtis, C. and Mark, N. 2024, GDP and Temperature: Evidence on Cross-Country Response Heterogeneity, *European Economic Review* **169**, 104833.
- Beveridge, S. and Nelson, C. R. 1981, A New Approach to Decomposition of Economic Time Series into Permanent and Transitory Components with Particular Attention to Measurement of the Business Cycle, *Journal of Monetary Economics*.
- Biaswas, E., Sabzikar, F. and Phillips, P. 2023, Boosting the HP Filter for Trending Time Series and Long Range Dependence, unpublished manuscript.
- Bilal, A. and Kanzig, D. 2024, The Macroeconomic Impact of Climate Change: Global vs Local Temperature, NBER Working paper 32450.
- Cameron, A. C., Gelbach, J. B. and Miller, D. L. 2011, Robust Inference With Multiway Clustering, *Journal of Business & Economic Statistics* **29(2)**, 238–249.
- Clark, P. 1987, The Cyclical Component of U.S. Economic Activity, *Quarterly Journal of Economics* **102:4**, 797–814.
- Dell, M., Jones, B. and Olken, B. 2014, What do we Learn from the Weather? The New Climate-Economy Literature, *Journal of Economic Literature* **52:3**, 740–798.
- Foerster, A., Hornstein, A., Sarte, P. and Watson, M. 2022, Aggregate Implications of Changing Sectoral Trends, *Journal of Political Economy* **130:12**, 3286–3330.
- Gil-Alana, L., Gupta, R., L.Sauci and Carmona-Gonzales, N. 2022, Temperature and Precipitation in the US States: Long Memory, Persistence, and Time Trend, *Theoretical and Applied Climatology* **150**, 1731–1744.
- Hamilton, J. D. 2018, Why You Should Never Use the Hodrick-Prescott Filter, *Review of Economics and Statistics* **100:5**, 831–843.
- Hartl, T. 2023, The Fractional Unobserved Components Model: A Generalization of Trend-Cycle Decompositions to Data of Unknown Persistence, unpublished manuscript.
- Harvey, A. C. 1994, *Time Series Models*, second edn, MIT Press, Oxford.
- Hodrick, R. and Prescott, E. 1997, Post-War U.S. Business Cycles: An Empirical Investigation, *Journal of Money Credit and Banking* **29**, 1–16.
- Hsiang, S. 2016, Climate Econometrics, *Annual Review of Resource Economics* **8**, 43–75.
- Hsiang, S. and Burke, M. 2014, Climate, Conflict, and Social Stability: What does the Evidence Say?, *Climate Change* **123**, 39–55.

- IPCC 2014, Climate Change 2014: Impacts, Adaptation and Vulnerability, *Contribution of Working Group II to the Fifth Assessment Report of the Intergovernmental Panel on Climate Change*, Vol. 1, Cambridge University Press, Cambridge.
- Kahn, M., Mohaddes, K., Ng, R., Pesaran, M. H., Rassi, M. and Yang, J. 2021, Long Term Macroeconomic Effects of Climate Change: A Cross-Country Analysis, *Energy Economics*.
- Kalkuhl, M. and Wenz, L. 2020, The Impact of Climate Conditions on Economic Production. Evidence from a Global Panel of Regions, *Journal of Environmental and Management* **103**, 102360.
- Kaufmann, R., Kauppi, H., Mann, M. and Stock, J. H. 2013, Does Temperature Contain a Stochastic Trend: Linking Statistical Results to Physical Mechanisms, *Climate Change* **118**, 729–743.
- Klosin, S. 2024, Dynamic Biases of Static Panel Data Estimators, unpublished manuscript.
- Kuttner, K. 1994, Estimating Potential Output as a Latent Variable, *Journal of Business and Economic Statistics* **12:3**, 361–368.
- Majerovitz, J. and Sastry, K. A. 2023, How Much Should We Trust Regional-Exposure Designs?, unpublished manuscript.
- Marino, M. and Marmol, F. 2004, A Permanent-Transitory Decomposition for ARFIMA Processes, *Journal of Statistical Planning and Inference* **124**, 87–97.
- Mills, T. 2007, Time Series Modelling of two Millennia of Northern Hemisphere Temperatures: Long Memory or Shifting Trends?, *Journal of the Royal Statistical Society Series A* **170:1**, 83–94.
- Mohaddes, K., Ng, R. N. C., Pesaran, M. H., Raissi, M. and Yang, J.-C. 2023, Climate Change and Economic Activity: Evidence from US States, *Oxford Open Economics* **2**, odac010.
- Mudelsee, M. 2019, Trend Analysis of Climate Time Series: A Review, *Earth Science Reviews* **190**, 310–322.
- Mueller, U. and Watson, M. W. 2008, Testing Models of Low-Frequency Variability, *Econometrica* **76**, 775–804.
- Mueller, U. and Watson, M. W. 2016, Measuring Uncertainty about Long-Run Predictions, *Review of Economic Studies* **83**, 1711–1740.
- Mueller, U. K. and Watson, M. W. 2017, Low Frequency Econometrics, *Advances in Economics and Econometrics*, Vol. 2, Cambridge University Press, p. p53.
- Mueller, U. K. and Watson, M. W. 2018, Long-Run Covariability, *Econometrica* **86:3**, 775–804.
- Mueller, U. K. and Watson, M. W. 2022, Low Frequency Analysis of Economic Time Series, *Handbook of Econometrics*, Vol. 7, North Holland, p. xxx.
- Nath, I., Ramey, V. and Klenow, P. 2024, How Much will Global Warming Cool Global Growth, NBER Working Paper 32761.
- Phillips, P. and Jin, S. 2021, Business Cycles, Trend Elimination and the HP Filter, *International Economic Review* **62**, 469:520.

- Phillips, P. and Shi, Z. 2021, Boosting: Why You Can Use the HP Filter, *International Economic Review* **62**, 521–570.
- Phillips, P. B. and Moon, H. 1999, Linear Regression Limit Theory for Nonstationary Panel Data, *Econometrica* **78:5**, 1057–1111.
- Ravn, M. and Uhlig, H. 2002, On Adjusting the Hodrick-Prescott Filter for the Frequency of Observations, *Review of Economics and Statistics* **84:2**, 371–380.
- Tol, R. 2024, A Meta Analysis of the Total Economic Impact of Climate Change, *Energy Policy* **185**, 113922.
- Tol, R. S. and Wagner, S. 2010, Climate Change and Violent Conflict in Europe over the Last Millennium, *Journal of Economic Perspectives* **99**, 65–79.
- Wu, Z., Huang, N., Long, S. and Peng, C. 2007, On the Trend, Detrending, and Variability of Nonlinear and Nonstationary Time Series, *Proceedings of the National Academy of Sciences* **104**, 14889–14894.
- Yuan, N., Fu, Z. and Liu, S. 2014, Extracting Climate Memory using Fractional Integrated Statistical Model: A New Perspective on Climate Prediction, *Nature* p. 6577.
- Zhang, D., Brecke, P., Lee, H., He, Y. and Zhang, J. 2007, Global Climate Change, War, and Population Decline in Recent Human History, **104:49**, 19214–19219.